LBNL-40267
UC-1501

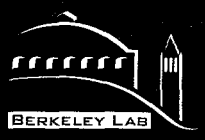

ERNEST ORLANDO LAWRENCE
BERKELEY NATIONAL LABORATORY

Exploratory Technology Research Program for Electrochemical Energy Storage

Annual Report for 1996

Kim Kinoshita, Editor

Environmental Energy Technologies Division

June 1997

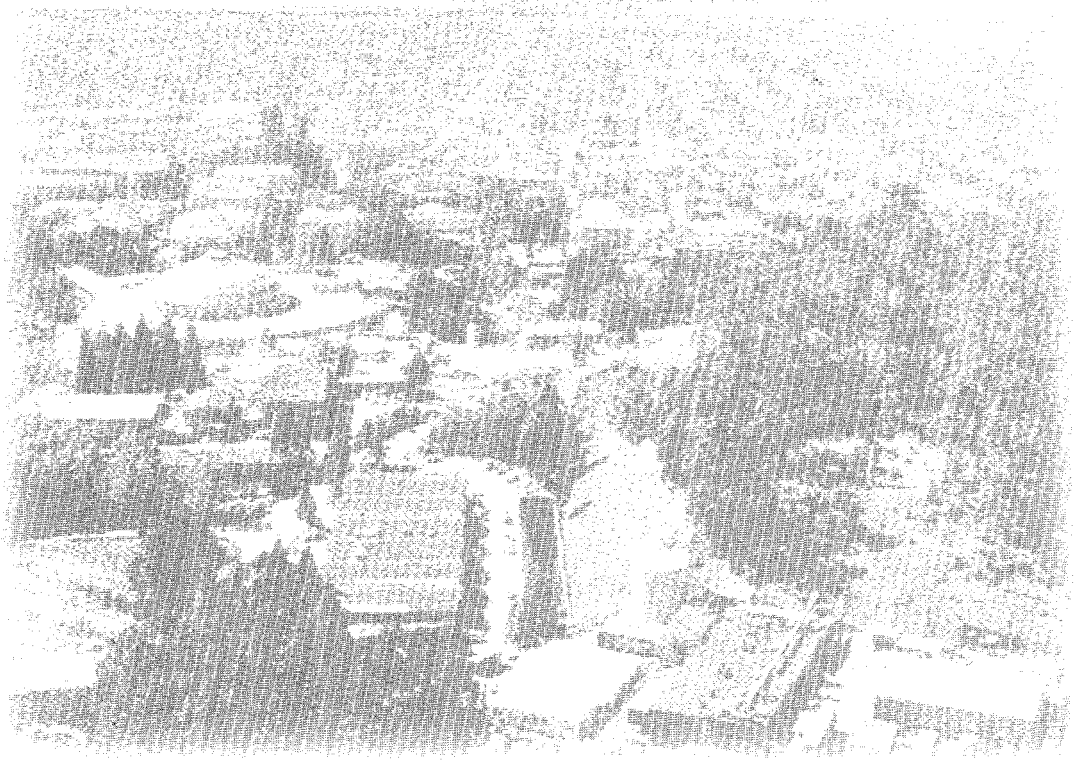

LBNL-40267

EXPLORATORY TECHNOLOGY RESEARCH PROGRAM FOR ELECTROCHEMICAL ENERGY STORAGE

ANNUAL REPORT FOR 1996

Environmental Energy Technologies Division
Lawrence Berkeley National Laboratory
University of California
Berkeley, California 94720

Edited by Kim Kinoshita, Technical Manager

June 1997

This work was supported by the Assistant Secretary for Energy Efficiency and Renewable Energy, Office of Transportation Technologies, Office of Advanced Automotive Technologies of the U.S. Department of Energy under Contract No. DE-AC03-76SF00098.

CONTENTS

C. COMPONENTS FOR AMBIENT-TEMPERATURE NONAQUEOUS CELLS

D. CROSS-CUTTING RESEARCH

IV. FUEL CELL RESEARCH

EXECUTIVE SUMMARY

The U.S. Department of Energy's Office of Transportation Technologies provides support for an Electrochemical Energy Storage Program, that includes research and development on advanced rechargeable batteries and fuel cells. A major goal of this program is to develop electrochemical power sources suitable for application in electric vehicles (EVs) and hybrid systems. The program centers on advanced electrochemical systems that offer the potential for high performance and low life-cycle costs, both of which are necessary to permit significant penetration into commercial markets.

The DOE Electric Vehicle Technology Program is divided into two project areas: the United States Advanced Battery Consortium (USABC) and Advanced Battery R&D which includes the Exploratory Technology Research (ETR) Program managed by the Lawrence Berkeley National Laboratory* (LBNL). The USABC, a tripartite undertaking between DOE, the U.S. automobile manufacturers and the Electric Power Research Institute (EPRI), was formed in 1991 to accelerate the development of advanced batteries for EVs. In addition, DOE is actively involved in the Partnership for a New Generation of Vehicles (PNGV) Program which seeks to develop passenger vehicles with a range equivalent to 80 mpg of gasoline. The role of the ETR Program is to perform supporting research on the advanced battery systems under development by the USABC and the PNGV Program, and to evaluate new systems with potentially superior performance, durability and/or cost characteristics. The specific goal of the ETR Program is to identify the most promising electrochemical technologies and transfer them to the USABC, the battery industry and/or other Government agencies for further development and scale-up. This report summarizes the research, financial and management activities relevant to the ETR Program in CY 1996. This is a continuing program, and reports for prior years have been published; they are listed at the end of this Executive Summary.

The general R&D areas addressed by the program include identification of new electrochemical couples for advanced batteries, determination of technical feasibility of the new couples, improvements in battery components and materials, establishment of engineering principles applicable to electrochemical energy storage and conversion, and the development of fuel cell technology for transportation applications. Major emphasis is given to applied research which will lead to superior performance and lower life-cycle costs.

The ETR Program is divided into three major program elements: Exploratory Research, Applied Science Research and Fuel Cell Research (no longer included in the ETR Program as of FY 1997). Highlights of each program element are summarized according to the appropriate battery system or electrochemical research area.

---

* Participants in the ETR Program include the following LBNL scientists: E. Cairns, J. Evans, K. Kinoshita, F. McLarnon and J. Newman of the Energy and Environment Division; and L. De Jonghe, P. Ross and C. Tobias (Professor Emeritus)** of the Materials Sciences Division.

** Professor Tobias died March 6, 1996.

EXPLORATORY RESEARCH

The objectives of this program element are to identify, evaluate and initiate development of new electrochemical couples with the potential to meet or exceed the electrochemical performance goals for advanced batteries and capacitors. Research was conducted on novel Na cells that contain polymer electrolytes, an all-solid state Li/Mn oxide cell and carbons for electrochemical double-layer capacitors.

- LBNL measured the conductivities, diffusion coefficients, and transference numbers for the PEO-NaTFSI system at 85°C and the PPO-LiTFSI system at 25°C, and the results show that transference numbers are (i) composition dependent and system specific, (ii) are universally non-unity at all salt concentrations and (iii) are negative for all but the most dilute solutions.
- Oak Ridge National Laboratory (ORNL) fabricated laboratory-scale solid-state cells with $LiMn_2O_4$ electrodes with open circuit voltages (OCVs) between 2.98 and 4.03 V, consistent with the cathode composition with $x \leq 1$ for $Li_xMn_2O_4$. Studies indicate that the cathode surface has undergone a phase change to the orthorhombic structure for $x > 1$ and the cell resistance increased as a result of the initial discharge.
- SAFT Research & Development Center built and tested cells with 140 F capacitance and 20 milliohms resistance, corresponding to high-performance capacitors delivering 6.1 Wh/kg and 3.9 Kw/kg.

APPLIED SCIENCE RESEARCH

The objectives of this program element are to provide and establish scientific and engineering principles applicable to batteries and electrochemical systems; and to identify, characterize and improve materials and components for use in batteries and electrochemical systems. Projects in this element provide research that supports a range of battery systems that contain solid electrolyte and nonaqueous electrolytes, both liquid and polymer. Other cross-cutting research efforts are directed at improving the understanding of electrochemical engineering principles, minimizing corrosion of battery components, and analyzing the surfaces of electrodes.

Electrode Characterization studies are an important research element for the successful development of rechargeable electrodes for advanced secondary batteries. Efforts are underway to evaluate the performance of cells utilizing Li intercalation electrodes, and use advanced spectroscopic techniques to investigate the chemical state of electrode materials during charge/discharge cycling.

- A process involving catalytic chemical vapor deposition (CVD) has been developed by LBNL to synthesize carbonaceous materials which have a reversible Li capacity of about 370 mAh/g.
- Lawrence Livermore National Laboratory (LLNL) investigated the Li intercalation capacities of petroleum needle cokes (190LS, Superior Graphite Co.) that were air milled and heat treated to

1800, 2100 or 2350°C. The highest Li intercalation capacity (x = 0.93 in Li_xC_6) was obtained with a sample that was heat treated at 2350°C and then air milled.

- Brookhaven National Laboratory (BNL) has fabricated new hermetically sealed spectroelectrochemical cells for *in situ* extended X-ray diffraction (XRD) and X-ray absorption spectroscopy (XAS) to study transition metal oxide cathodes for Li cells. EXAFS showed that the spinel structure of $LiMn_2O_4$ changed less than that of $LiNiO_2$ during the first charge.

Electrodes for Electrochemical Cells are being developed to identify low-cost metal hydrides for metal-hydride cells and improved metal oxides for electrochemical capacitors.

- BNL demonstrated that the presence of cobalt and aluminum in AB_5 hydride electrodes strongly inhibits corrosion by reducing the lattice expansion and contraction in the electrochemical charge-discharge process, and in the case of Co, by the formation of a corrosion-resistant surface layer.
- The University of South Carolina has observed that microencapsulation of hydrogen storage alloys with electroless nickel or cobalt-nickel coatings improved the cycle life by forming a conductive passive film on the surface which prevents unwanted oxidation of the active materials.
- The University of Michigan has developed a novel network-generation approach which was validated with experimental resistivities in fibrous substrates. A new mechanics technique has also been developed to model the damage progression in the fibrous substrates.
- The University of Wisconsin successfully fabricated thin-film capacitor cells using nickel oxide thin-film electrodes. The specific energy, specific power and volumetric energy density (based on only the active material) obtained from a single cell with nonaqueous electrolyte were 11.85 Wh/kg, 1200 W/kg and 16.9 Wh/liter, respectively.

Components for Ambient-Temperature Nonaqueous Cells, particularly metal/electrolyte combinations that improve the rechargeability of these cells, are under investigation.

- LBNL demonstrated greatly improved utilization of the sulfur active material in the range of 40% and higher in Li/S cells.
- LBNL has observed that tungsten-implanted Al is highly resistant to pitting corrosion during repeated potentiodynamic scans and during cycle tests in Li/V_6O_{13} cells.
- Northwestern University synthesized polymer electrolytes based on $[PN(OCH_2CH_2OCH_2CH_2OCH_3)_2]_n$ (MEEP), which showed better cell performance than aluminosilicate-polyether hybrid electrolytes, but cell capacity declined rapidly during cycling.
- Northwestern University developed a general method for analysis of ion dynamics during energy-conversion cycles, including redox properties at the electrode/electrolyte interface.
- Cycling studies of $Li_xM_yMnO_2$ (M = Li, Na, K) at the State University of New York (Binghamton) showed that the highest capacity and longest life was obtained when M = K, which provided the largest interlayer spacing.

- Covalent Associates Inc. fabricated test cells with $LiCr_{0.02}Mn_{1.98}O_4/LiPF_6$-EC:DEC/Li foil which achieved an initial discharge capacity of 118 mAh/g, falling to 105 mAh/g after 486 cycles, when the cell failed. This project has been completed.

Cross-Cutting Research is carried out to develop mathematical models of electrochemical systems and to address fundamental phenomenological problems; solutions will lead to improved electrode structures and better performance in batteries and fuel cells.

- LBNL has used slow charge/discharge potential transients, cyclic voltammetry, and potential-step transients using a hydrogen nickel hydroxide thin-film cell to obtain data to verify a numerical model that considers contributions of charge-transfer resistance, mass-transfer limitations, and side reactions.
- Quantitative analysis of the surface-enhanced Raman (SER) spectra of a $Ni/Ni(OH)_2$ electrode by LBNL showed that the initial α-$Ni(OH)_2$ phase is only partially converted into β-$Ni(OH)_2$ during cycling.

FUEL CELL RESEARCH

The objectives of this program element are to characterize and improve materials for fuel cells for transportation applications. This research includes projects in several areas of electrochemistry: fuel-cell testing, fuel processing, fuel-cell component characterization and theoretical studies. Fuel cell research is not included in the ETR Program as of FY 1997. Major achievements of the fuel-cell program during 1996 are listed below:

- LBNL has determined that both the surface and bulk composition of $Pt_{75}Mo_{25}$ alloy for hydrogen oxidation was the same.
- LBNL has made major advances in eliminating the unwanted coupling of the nuclear magnetic resonance (NMR) sample to the coil, thereby permitting the acquisition of meaningful NMR spectra of fuel-cell electrode surface species under open-circuit conditions and strongly suggesting the possibility of acquiring spectra under conditions of *in situ* electrode potential control.
- Los Alamos National Laboratory (LANL) has demonstrated a proof of concept for using the hydrophilic domains in a composite backing material for membrane-electrode assemblies (MEAs).
- LANL was able to lower the methanol cross-over rate at 80°C from 110 mA_{eq}/cm^2 through a standard Nafion® 117 membrane to 40 mA_{eq}/cm^2 by use of an alternative membrane.
- LANL has demonstrated that continuous stable operation of direct methanol fuel cells (DMFCs) for 500 h is achievable by modifying the cathode structure.

MANAGEMENT ACTIVITIES

During 1996, LBNL managed 13 subcontracts and conducted a vigorous research program in electrochemical energy storage. LBNL staff members attended project review meetings, made site visits to subcontractors, and participated in technical management of various ETR projects. LBNL staff members also participated in the following reviews, meetings, and workshops:

10th International Conference on Solid State Ionics, Singapore, December 3-8, 1995

188th Meeting of the Electrochemical Society, Chicago, IL, October 8-13, 1995

DOE OTT/BES Review Meeting, Berkeley, CA, March 26-27, 1996

189th Meeting of the Electrochemical Society, Los Angeles, CA, May 5-10, 1996

Gordon Conference on Solid State Ionics, New London, NH, June 16-21, 1996

8th International Meeting on Lithium Batteries, Nagoya, Japan, June 16-22, 1996

31st IECEC, Washington D.C., August 11-15, 1996

47th International Society of Electrochemistry, Veszprem and Balatonfürad, Hungary, September 1-6, 1996

190th Meeting of the Electrochemical Society, San Antonio, TX, October 6-11, 1997

1996 Automotive Technology Development Customers' Coordination Meeting, Dearborn, MI, October 28-November 1, 1996

ACKNOWLEDGMENT

This work was supported by the Assistant Secretary for Energy Efficiency and Renewable Energy, Office of Transportation Technologies, Office of Advanced Automotive Technologies of the U.S. Department of Energy under Contract No. DE-AC03-76SF00098. The support from DOE and the contributions by the participants in the ETR Program are acknowledged. The assistance of Ms. Susan Lauer for coordinating the publication of this report and Mr. Garth Burns for providing the financial data are gratefully acknowledged.

ANNUAL REPORTS

1. Exploratory Technology Research Program for Electrochemical Energy Storage – Annual Report for 1995, LBNL-338842 (June 1996).

2. Exploratory Technology Research Program for Electrochemical Energy Storage – Annual Report for 1994, LBL-37665 (September 1995).

3. Exploratory Technology Research Program for Electrochemical Energy Storage – Annual Report for 1993, LBL-35567 (September 1994).

4. Exploratory Technology Research Program for Electrochemical Energy Storage – Annual Report for 1992, LBL-34081 (October 1993).

5. Exploratory Technology Research Program for Electrochemical Energy Storage – Annual Report for 1991, LBL-32212 (June 1992).

6. Technology Base Research Project for Electrochemical Energy Storage – Annual Report for 1990, LBL-30846 (June 1991).

7. Technology Base Research Project for Electrochemical Energy Storage – Annual Report for 1989, LBL-29155 (May 1990).

8. Technology Base Research Project for Electrochemical Energy Storage – Annual Report for 1988, LBL-27037 (May 1989).

9. Technology Base Research Project for Electrochemical Energy Storage – Annual Report for 1987, LBL-25507 (July 1988).

10. Technology Base Research Project for Electrochemical Energy Storage – Annual Report for 1986, LBL-23495 (July 1987).

11. Technology Base Research Project for Electrochemical Energy Storage – Annual Report for 1985, LBL-21342 (July 1986).

12. Technology Base Research Project for Electrochemical Energy Storage – Annual Report for 1984, LBL-19545 (May 1985).

13. Annual Report for 1983 – Technology Base Research Project for Electrochemical Energy Storage, LBL-17742 (May 1984).

14. Technology Base Research Project for Electrochemical Energy Storage – Annual Report for 1982, LBL-15992 (May 1983).

15. Technology Base Research Project for Electrochemical Energy Storage – Report for 1981, LBL-14305 (June 1982).

16. Applied Battery and Electrochemical Research Program Report for 1981, LBL-14304 (June 1982).

17. Applied Battery and Electrochemical Research Program Report for Fiscal Year 1980, LBL-12514 (April 1981).

LIST OF ACRONYMS

AES	Auger electron spectroscopy
BET	Brunauer-Emmett-Teller
BNL	Brookhaven National Laboratory
CPE	composite polymer electrolyte
CVD	chemical vapor deposition
DMC	dimethyl carbonate
DME	dimethoxyethane
DMF	dimethylformamide
DMFC	direct methanol fuel cell
DOE	Department of Energy
EC	ethylene carbonate
EDS	energy dispersive spectroscopy
EDX	energy dispersive X-ray analysis
EPRI	Electric Power Research Institute
ESCA	electron spectroscopy for chemical analysis
ETR	Exploratory Technology Research
EV	electric vehicle
EXAFS	extended X-ray absorption fine structure
FTIR	Fourier transform infrared spectroscopy
HREM	high-resolution electron microscopy
HRTEM	high-resolution transmission electron microscopy
IECEC	Intersociety Energy Conversion Engineering Conference
INEL	Idaho National Engineering Laboratory
ISE	International Society of Electrochemistry
LANL	Los Alamos National Laboratory
LBNL	Lawrence Berkeley National Laboratory
LEED	low-energy electron diffraction
LEIS	low-energy ion scattering
Lipon	lithium phosphorous oxygen nitrogen
LLNL	Lawrence Livermore National Laboratory
MEA	membrane-electrode assembly
NMR	nuclear magnetic resonance
NSLS	National Synchrotron Light Source
OCV	open circuit voltage
ORNL	Oak Ridge National Laboratory
PAN	polyacrylonitrile
PC	propylene carbonate
PDS	photothermal deflection spectroscopy
PEFC	polymer electrolyte fuel cells

PEG	polyethylene glycol
PEO	polyethylene oxide
PNGV	Partnership for a New Generation of Vehicles
PPO	polydimethylphenylene oxide
PTFE	polytetrafluoroethylene
PVDF	polyvinylidene difluoride
rf	radio frequency
SEM	scanning electron microscopy
SERS	surface-enhanced Raman spectroscopy
TEM	transmission electron microscopy
TFSI	trifluorosulfonylimide
THF	tetrahydrofuran
TMA	tetramethyl ammonium
UHV	ultrahigh vacuum
USABC	United States Advanced Battery Consortium
XANES	X-ray absorption near-edge spectroscopy
XAS	X-ray absorption spectroscopy
XRD	X-ray diffraction

SUBCONTRACTOR FINANCIAL DATA - CY 1996

Subcontractor	Principal Investigator	Project	Contract Value (K$)	Term (months)	Expiration Date	Status in CY 1996*
EXPLORATORY RESEARCH						
Solid-State Cells						
Oak Ridge National Laboratory	J. Bates	Rechargeable Li Batteries	65	12	9-96	C
Electrochemical Double-Layer Capacitors						
SAFT America, Inc.	G. Chagnon	Novel Cell Components	115	12	12-97	C
APPLIED SCIENCE RESEARCH						
Lawrence Berkeley National Laboratory	E. Cairns, L. DeJonghe, J. Evans, K. Kinoshita, F. McLarnon, J. Newman, P. Ross**	Electrochemical Energy Storage	1980	12	9-96	C
Electrode Characterization						
Lawrence Livermore National Lab.	T. Tran	Li-Ion Carbon Electrode	70	12	9-96	C
Brookhaven National Laboratory	J. McBreen	Battery Materials	140	12	9-96	C
Electrodes for Electrochemical Cells						
Brookhaven National Laboratory	J. Reilly	Metal Hydride Electrodes	185	12	9-96	C
University of South Carolina	R. White	Metal Hydride Properties	90	12	9-97	C
University of Michigan	A.M. Sastry	Novel Cell Components	80	12	8-97	C
University of Wisconsin	M. Anderson	Sol-Gel Derived Metal Oxides	120	12	8-97	C
Components for Ambient-Temperature Nonaqueous Cells						
Northwestern University	M. Ratner	Polymer Electrolytes	145	12	10-97	C
Northwestern University	D. Shriver	Polymer Electrolytes	113	12	3-96	T
SUNY at Binghamton	S. Whittingham	Cathode Materials	70	12	5-97	C
Covalent	W.F. Howard	Li Polymer Batteries	250	18	8-96	T
FUEL CELL RESEARCH						
Fuel Cell R&D						
Los Alamos National Laboratory	S. Gottesfeld**	Fuel Cell R&D	1450	12	9-96	C**

* C = continuing, T = terminating

** Fuel Cell Research not included in ETR Program as of FY 1997

I. INTRODUCTION

This report summarizes the progress made by the Exploratory Technology Research (ETR) Program for Electrochemical Energy Storage during calendar year 1996. The primary objective of the ETR Program, which is sponsored by the U.S. Department of Energy (DOE) and managed by Lawrence Berkeley National Laboratory (LBNL), is to identify electrochemical technologies that can satisfy stringent performance, durability and economic requirements for electric vehicles (EVs). The ultimate goal is to transfer the most-promising electrochemical technologies to the private sector or to another DOE program for further development and scale-up. Besides LBNL, which has overall responsibility for the ETR Program, LANL, LLNL, ORNL and BNL have participated in the ETR Program by providing key research support in several of the program elements. The ETR Program consists of three major elements:

Exploratory Research

Applied Science Research

Fuel Cell Research

The objectives and the specific battery and electrochemical systems addressed by each program element are discussed in the following sections, which also include technical summaries that relate to the individual programs. Financial information that relates to the various programs and a description of the management activities for the ETR Program are described in the Executive Summary.

II. EXPLORATORY RESEARCH

The major thrust of this program element is to evaluate promising electrochemical couples for advanced batteries for EVs. Exploratory research was conducted on novel Na cells that contain polymer or molten-salt electrolytes, an all-solid state Li/Mn oxide cell and carbons for electrochemical double-layer capacitors.

A. SOLID-STATE CELLS

Efforts are underway to develop all-solid-state cells. The studies focus on demonstrating the viability of a sodium/sodium-alloy negative or a lithium negative and a metal oxide positive or an organosulfur positive in a rechargeable cell. In addition, the feasibility of an ambient-temperature molten-salt electrolyte cell was investigated.

Solid Electrolytes

Lutgard C. De Jonghe
62-203, Lawrence Berkeley National Laboratory, Berkeley CA 94720
(510) 486-6138, fax: (510) 486-4881

Objectives

- Fabricate and study novel composite electrolytes which combine the advantages of a protective thin-film single-ion conductor with a conventional elastomeric polymer electrolyte for EV applications.
- Develop a suitable composite electrolyte material for use in alkali metal/polymer cells.

Approach

- Synthesize and characterize a Li single-ion conductor combined in a single composite membrane acting as a separator in rechargeable Li batteries.
- Employ AC and DC techniques (*e.g.*, galvanostatic charging and discharging, four-probe techniques, impedance spectroscopy and pulse testing) and thermal measurements to characterize solid-state batteries, as well as the properties of the individual components and interfaces.

Accomplishments

- A study of the transport properties of PEO-NaTFSI (TFSI=$N(CF_3SO_2)_2$) electrolytes was completed.
- Thin solid films of $Li_{3x}La_{0.67-x}TiO_3$ were prepared by hydraulically pressing powders under an inert atmosphere.

Future Directions

- Expand research on ceramic single-ion conductors and parallel and series composite membranes.
- Prepare and test parallel composite membranes containing $Li_{3x}La_{0.67-x}TiO_3$ and PEO.
- Carry out further work on transport properties of polymer electrolytes under this project and under a new initiative with J. Kerr.

The goals of the present research program are to fabricate and study novel composite electrolytes which combine the advantages of a single-ion conductor with a conventional elastomeric polymer electrolyte. The configuration may be either in a series (thin-film layers) or parallel form (single-ion conductor dispersed within a polymer matrix). Emphasis is placed on potentially low-cost, conventional approaches to extending the cycle life of alkali metal/polymer batteries. Fundamental investigations of bulk, composite and thin-film electrolytes will be conducted to furnish information on the electrochemical, thermal and mechanical properties of these polymer-based materials, and provide the basis for advanced design of batteries with improved safety features and longer cycle lives.

Conductivities, diffusion coefficients, and transference numbers for the PEO-NaTFSI system at 85°C and the PPO-LiTFSI system at 25°C were obtained. These data show that transference numbers are composition dependent and system specific. Transference numbers are universally non-unity at all salt concentrations and are negative for all but the most-dilute solutions. This is a consequence of the non-ideality of the polymer-salt solutions and indicates that transport occurs primarily *via* negatively charged ionic complexes rather than by free ions. The existence of such complexes was confirmed by recent Raman spectroscopic results obtained on PEO-$NaCF_3SO_3$ solutions at Umeå University (Sweden) as a result of a recent collaboration with our group. Our results suggest that the difficulties researchers have encountered in attempting to develop polymeric single-ion conductors may, in fact, be due to the low mobility of uncomplexed Li ions.

T_0^+ exhibits a minimum at an O:M ratio of 70:1 in the PPO-LiTFSI system that coincides with a maximum in conductivity and salt diffusion coefficient. At low salt concentrations, there is a high concentration of free cations but they interact strongly with OH end groups in the polymer and are relatively immobile. At high salt concentrations, the preponderance of large ion aggregates renders the system sluggish. The

highest ratio of mobile species exists at an O:M ratio of 70:1; the -2.3 value of t_0^+ strongly implies that this is a negatively charged triplet. The relative invariance of t_0^+ with salt concentration in the PEO-NaTFSI system is an advantage for this system over that of the highly composition-dependent PEO-$NaCF_3SO_3$ system. Experiments on $Na/PEO\text{-}NaTFSI/Na_xMnO_2$ cells show that performance is relatively insensitive to the PEO-NaTFSI electrolyte composition. This is in marked contrast to the PEO-$NaCF_3SO_3$ system; salt precipitation causes premature failure of operating cells when concentrated salt solutions are used as electrolytes. The reasons for the differing behaviors of these two systems are unknown; a further investigation into what determines transport behavior in polymer-salt systems will be relevant for design of next-generation polymer electrolytes.

Polyacrylonitrile (PAN) electrolytes containing $LiClO_4$ or LiTFSI and propylene carbonate/ethylene carbonate mixtures were also studied. While conductivities at room temperature were high (>10^{-3} S/cm), cyclic voltammetry experiments indicated that a rapid reaction with metallic Li occurs, increasing the interfacial resistance markedly. This reaction can be prevented completely by placing a disk of Li_3N between the anode and the electrolyte. Randomly oriented hot-pressed disks of Li_3N had ionic conductivities of 8×10^{-5} S/cm at room temperature, close to the theoretical value found for single crystals ($\sigma_\perp = 2 \times 10^{-5}$ S/cm, $\sigma_{||} = 1 \times 10^{-3}$ S/cm). While these preliminary results were promising, the thickness of the hydraulically pressed disks could not be reduced below about 500 μm, leading to an unacceptably high internal cell resistance. General Vacuum Equipment has recently agreed to provide Li surface-treated with thin (1000Å or less) films of vacuum-deposited lithium nitride for evaluation. This should allow further testing of the concept of series composite electrolytes to proceed.

Synthesis of smectic clay-PEO nanocomposites is also underway. Smectic clays consist of charged alumino-silicate layers between which Na ions and water are inserted. Two systems are presently being examined: montmorillonite, a naturally occurring clay, and laponite, a synthetic ultra-pure clay produced by Southern Clay Company (Gonzales, TX). Because of the higher purity level, laponite is preferable for use in battery applications. Both clays are naturally single-ion conductors, although conductivities are typically too low for practical applications. Recent research by Lerner et al. at Oregon State University shows, however, that conductivities are enhanced 2-3 orders of magnitude by incorporation of PEO between the layers due to the increase in gallery spacings. Prior to use in electrochemical systems, the clay must be purified, ion-exchanged (Li for Na) and dried to remove water. It is then suspended in acetonitrile and PEO is added. At a weight ratio of ~0.3 g PEO per g of clay, nanocomposites self-assemble. The product may then be filtered and dried. X-ray diffraction (XRD) may be used to determine the inter-layer spacings; a significant increase in 00ℓ d-spacings is a positive confirmation that PEO has been inserted between the alumino-silicate layers. The XRD pattern of a laponite-PEO nanocomposite film, first produced in our laboratory, shows that the interlayer spacing of 19-20 Å is increased ~10Å over that of the native material. The films are tough, flexible and transparent. The presence of only 00ℓ lines indicates a high degree of preferred orientation for films of this material. Unfortunately, the orientation of the conducting planes is parallel to the substrate surface, leading to low ionic conductivities. Methods for changing the orientation and improving the conductivities are underway.

$Li_{3x}La_{0.67-x}TiO_3$ was synthesized by sintering isostatically pressed pellets at 1300°C for AC conductivity measurements. Future plans are to incorporate this material in a parallel composite electrolyte configuration, by coating small particles with PEO to overcome the high grain-boundary resistance.

PUBLICATIONS

P.I. Stallworth, S. Greenbaum, M.M. Doeff, Y. Ma, L. Ding and S. Visco, "^{23}Na NMR Studies of Na_xCoO_2 Cathode Materials," *Solid State Ionics*, **86-88**, 797 (1996).

A. Ferry, M.M. Doeff and L.C. De Jonghe, "Transport Property Measurements of Polymer Electrolytes," LBNL-39339, September, 1996.

M.M. Doeff, A. Ferry, Y. Ma, L. Ding and L.C. De Jonghe, "Effect of Electrolyte Composition on the Performance of Sodium/Polymer Cells," LBNL-39520, October, 1996.

M.M. Doeff, M. Peng, Y. Ma, S.J. Visco and L.C. De Jonghe, "Secondary Cell with Orthorhombic Alkali Metal/Manganese Oxide Phase Active Cathode Material," *U.S. Patent 5,558.961*, Sept. 24, 1996.

Development of a Thin-Film Rechargeable Lithium Battery for Electric Vehicles

John B. Bates
MS 6030, Oak Ridge National Laboratory, P.O. Box 2008, Oak Ridge TN 37830-6030
(423) 574-6280, fax: (423) 574-4143

Objectives

- Identify methods for depositing, at temperatures below 180°C, acceptable thin-film $Li_xMn_2O_4$ positive electrodes for rechargeable thin-film Li batteries.
- Develop solid-state Li/$Li_xMn_2O_4$ rechargeable batteries for EV applications that meet or exceed the long-term goals of the USABC.

Approach

- Fabricate $Li_xMn_2O_4$ electrodes at temperatures below 180°C by radio frequency (rf) magnetron sputtering using different process variables and substrate bias.
- Fabricate and test 4 V thin-film solid-state Li cells with $Li_xMn_2O_4$ (x<1) positive electrodes.
- Fabricate and test hybrid cells consisting of bulk-processed $LiMn_2O_4$ electrode plates, a thin LiPON electrolyte film and a thick Li anode film.

Accomplishment

- The least-resistive cells with $LiMn_2O_4$ electrodes were obtained by low-pressure deposition with a positive substrate bias.

Future Directions

- Increase the green density of $LiMn_2O_4$ tapes thereby allowing denser cathodes to be formed with much less grain growth.
- Fabricate significantly thinner tapes <40 μm.

The objective of this program is to fabricate a $LiMn_2O_4$ cathode in the form of a very thin flexible ceramic ribbon which would function not only as the cathode, but also as the support for the vapor-deposited solid electrolyte and the Li metal anode. This solid-state rechargeable Li battery, when operated at 60–100°C, is predicted to have the energy and power densities required for EV applications.

To date, cathode tapes 30–150 μm thick have been fabricated from an aqueous slip by tape casting and sintering techniques. Slips have been prepared using $LiMn_2O_4$ powder purchased from both Covalent (Woburn, MA) and Cerac (Milwaukee, WI). A number of different sintering conditions have been investigated to evaluate and optimize the microstructure and density of the cathodes. All-solid-state cells have been fabricated by sputter deposition of the lithium phosphorous oxynitride electrolyte ('Lipon' developed at ORNL) onto the sintered $LiMn_2O_4$ tapes, along with a Ni current collector and evaporated Li anode. The Lipon forms a crack-free uniform film which completely coats the rather rough surface of the sintered tapes. These cells were both charged and discharged at temperatures 50-100°C and current densities up to 100 $\mu A/cm^2$. So far the capacity of the cathode tapes appears to be limited to that of surface grains and cycling is impeded by a rapid increase in the cell resistance. These difficulties are believed to be due to the low density and poor connectivity of the cathode grains in the tapes fabricated to date.

The powder from Covalent has a narrower size distribution and near-spherical grains and agglomerates. It is slightly Li deficient and has 0.3 wt% Cr. The Cerac particles are more irregular and chunky which facilitates the particle packing as shown in Table 1. Both powders are routinely dry ball milled to reduce the agglomerates before formulating the slips. Investigations with cold-pressed pellets indicate that the highest green densities are obtained with the milled powders and that there is no significant advantage to be found in using mixtures of either the as-received + milled powders or the Covalent + Cerac powders.

Stable aqueous slips were formed using the milled powders, a polyacrylic acid dispersant (pH adjusted to 8.5) and an acrylic emulsion binder. The amount of binder was minimized to that needed in order to handle the green tape; more binder was required for the thinner castings. Typically the

slips were ~78 wt% total solids and ~37 vol% $LiMn_2O_4$. The tapes were cast on silicone-coated mylar at thicknesses of 40-200 μm. Burnout of the organics was complete at 550°C.

The tapes were sintered under flowing oxygen in a sealed tube furnace. If sintered in air, the $LiMn_2O_4$ is gradually reduced forming Mn_3O_4, whereas the spinel phase is maintained at 1 atm O_2 with only a small decrease in the lattice constant, 8.241(1)Å *vs.* 8.238(1)Å, for the as-received powder and sintered tape, respectively.

Tapes were characterized by their bulk density (*i.e.*, volume from geometric dimensions) and by scanning electron microscopy (SEM) examination. Figure 1 shows the micro-structure and density evolution with sintering temperature. At temperatures as low as 850°C, the grains have already begun to coarsen and become faceted, without any significant densification of the body. Several different sintering schemes have been tried to promote the bulk diffusion processes needed for densification over the competing surface or vapor transport which result in coarsening without shrinkage. These have included: very rapid heating rates, variation of the oxygen stoichiometry, presence of a higher-temperature $LiMn_2O_4$ vapor source, and addition of a small amount of a Li salt as a flux to draw the particles closer together. None of these techniques appear very promising. We plan to continue investigating various sintering schemes, but a major improvement will likely require a reformulation of the slip to achieve a higher green density. Current green densities are reasonably good, as for most ceramics ~50% is considered to be sufficient to achieve a dense sintered body with no open or continuous porosity, however, because the sintered density is generally found to depend strongly on the green density, efforts to improve the green densities will be pursued in future work.

Figure 2 shows several fracture cross sections of sintered tapes. Transgranular fracture is observed for tapes sintered to >3.5g/cm³. Even after prolonged sintering at 1200°C (Figs. 2a and 2b), there are still deep open pores at the surface and large intergranular pores within the bulk. The 70 μm thick tape shown in Fig. 2c is of the same material as that used to prepare the solid-state batteries discussed below. This tape is twice as thick as the targeted thickness, and more importantly the large pores between the grains will very likely weaken the material and impede the uniform conduction of Li through the cathode material.

Solid-state cells were fabricated by: (1) sputter deposition of 0.5 μm Ni on the back surface of the sintered tape, (2) sputter deposition of ~3 μm Lipon electrolyte on the front surface, and (3) vapor deposition of 10–25 μm thick Li as an island centered on the Lipon. The tapes were robust enough to withstand the film depositions without curling or cracking. Figures 3b and 3c show the Lipon coverage over the tape; Lipon forms a uniform coating over the surface features, bridging rather than filling the deep pores between the grains. Although a smoother tape would be preferable, the Lipon electrolyte forms a good separator. Cells have been stored for weeks without any observable change in the Li appearance or in the cell open circuit voltage (OCV). Significant short-circuit currents through the electrolyte would lead to a reduction in the OCV and/or an obvious thinning of the Li anode. New cells have OCVs between 2.98 and 4.03 V, consistent with the cathode composition with $x \leq 1$ for $Li_xMn_2O_4$.

Table 1. Densities (g/cm³) and (% of theoretical) for $LiMn_2O_4$*

	As-received powders			Dry milled powders					
Powders	Tap†	Pressed pellets		Pressed pellet		Green Tape‡		Sintered Tape**	
Cerac	1.54	–	–	2.92	(68%)	2.4	(55%)	4.0	(93%)
Covalent	1.01	2.5	(58%)	2.60	(60%)	2.0	(47%)	3.6	(84%)

* Theoretical density of $LiMn_2O_4$ is 4.3 g/cm³.

† Tap density from powder vibrated in a graduated cylinder.

‡ Excludes binder.

** Sintered at 1200°C in flowing O_2 for 10 h.

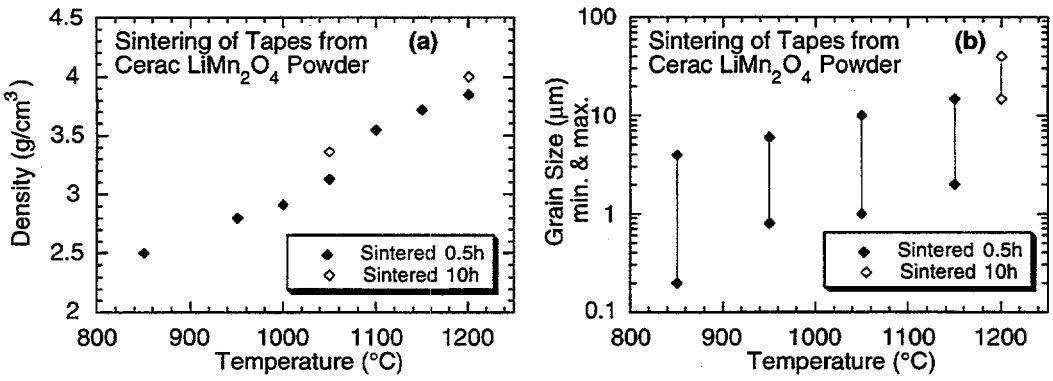

Figure 1. Bulk density and grain size distribution for sintered tapes prepared from dry milled Cerac $LiMn_2O_4$ powder. Heating rates were 10-20°C/m; cooling rates 1–10°C/m.

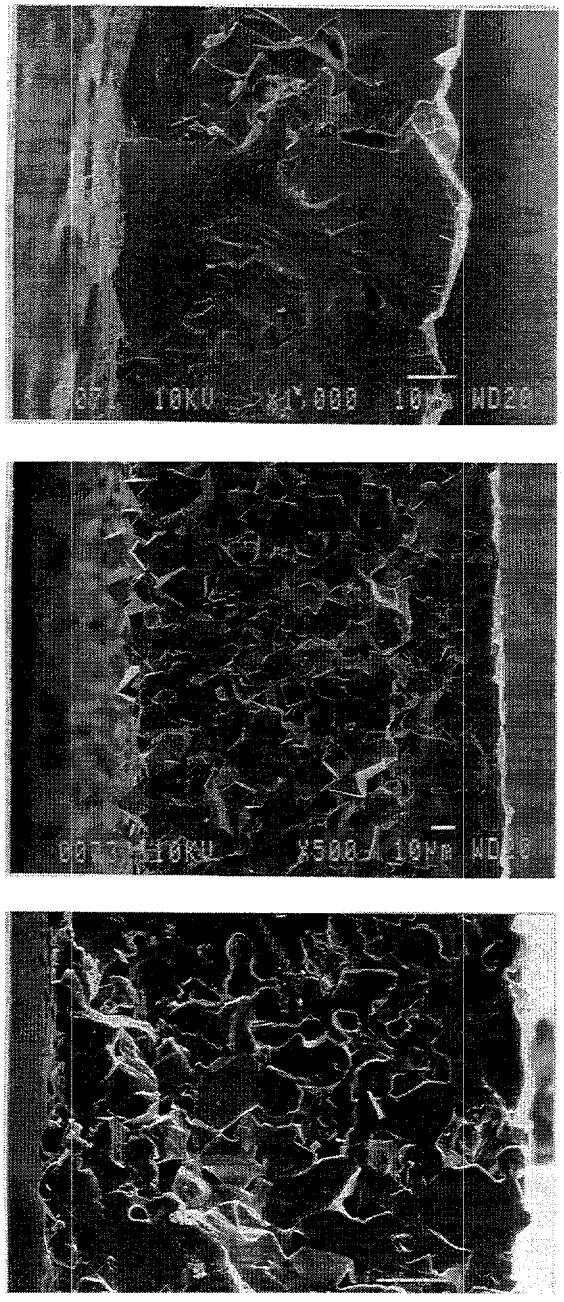

Figure 2. Fracture cross sections of sintered tapes. The tapes in (a) and (b) were prepared from Cerac and Covalent powder, respectively, and were both sintered at 1200°C for 10 h. The tape in (c) was from the Cerac powder and was sintered at 1150°C for 0.5 h. Magnifications are 1000X for (a), 500X for (b), and 1500X for (c).

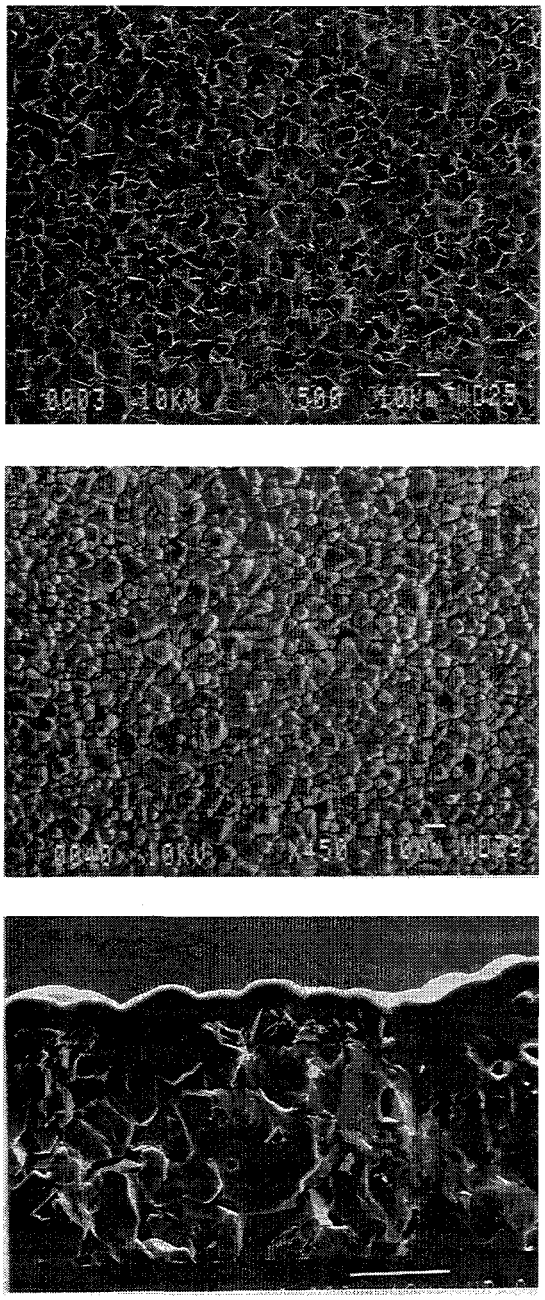

Figure 3. (a) Surface of $LiMn_2O_4$ tapes as-sintered and (b) after deposition of ~3 μm Lipon electrolyte. (c) Fracture cross section of Lipon-coated tape. The tapes were prepared from Cerac powder and sintered at 1150°C for 0.5 h. Magnifications are 500X for (a), 450X for (b), and 2000X for (c).

For cycling experiments, the cells were usually sealed in a stainless steel bottle with electrical feedthroughs. Contact to the Ni and Li was made using tantalum springs. AC impedance measurements at 25°C for uncycled cells indicate a cell resistance consistent with expected values based on our much-thinner vapor-deposited thin-film $LiMn_2O_4$ cells. Cells were charged and discharged at 50–100°C. Figure 4a shows the cell voltage at 100°C upon the initial charge. Between each charge step to 4.8 V the cell was allowed to relax. It is clear from the shape of the curve that the cell resistance increases by about an order of magnitude during the charge process from an initial value of ~500 $\Omega \cdot cm^2$. The total charge, ~0.21 mAh, corresponds to removal of ~16% of the Li in the cathode tape. Figure 4b shows a cell initially discharged at a low current density, followed by a recharge to 4.5 V. The 2 V plateau upon discharge indicates that the cathode surface has undergone a phase change to the orthorhombic structure for $x > 1$. Again the cell resistance increased as a result of the initial discharge. The increase in cell resistance has made it impossible so far to achieve more than several cycles with any of the cells. The cause of the resistance increase is not clear at this point. We suspect that the poor connection between the grains due to the low density may be responsible, but there is also some evidence that the grains themselves fracture upon the addition or removal of the Li. In either case, tapes which are both denser and finer grained may eliminate the source of the excessively high resistance.

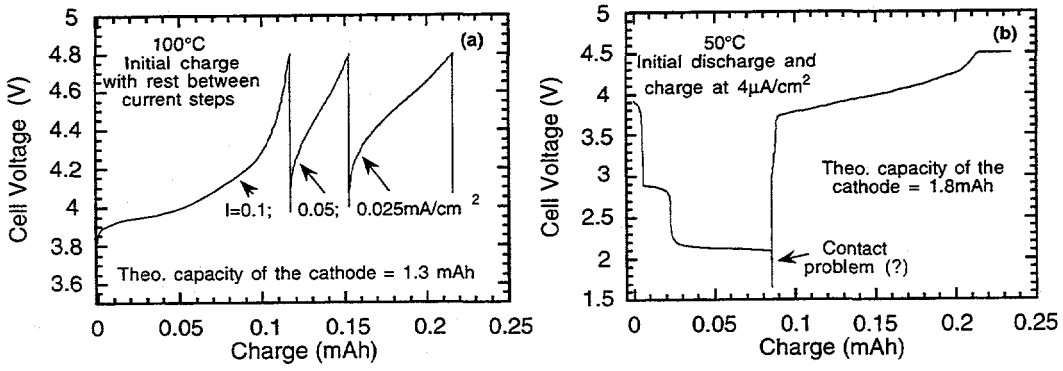

Figure 4. Cell voltage of $LiMn_2O_4$/Lipon/Li cells during initial charge (a) or initial discharge/charge (b). The test temperature and current densities are indicated in the figure. Both batteries were fabricated from a 70 μm thick Cerac $LiMn_2O_4$ tape sintered at 1150°C for 0.5 h.

B. ELECTROCHEMICAL DOUBLE-LAYER CAPACITORS

Research was initiated to evaluate carbons for electrochemical double-layer capacitors which can be used in EVs. Carbons are attractive electrode materials for capacitors because of their low cost relative to that of metal oxides which are commonly used.

Novel Cell Components for Capacitors

Guy Chagnon
SAFT Research & Development Center, 107 Beaver Court, Cockeysville, MD 21030
(410) 771-3200, fax: (410) 771-0234

Objectives

- Evaluate the double-layer capacitance of high-surface-area carbons.
- Develop low-cost carbon electrodes for electrochemical double-layer capacitors that meet the DOE goal of 1600 W/kg, 10 Wh/kg and $1/kW.

Approach

- Identify commercially available carbons for double-layer capacitors.
- Evaluate carbon electrode performance in "18650" test cells.

Accomplishments

- Polyvinyl alcohol was selected from the various binders for fabricating the carbon electrodes.
- Maxsorb (Mesocarbon) was selected from the various carbons for electrodes.
- Several cells were built with 140 F capacitance and 20 milliohms resistance, corresponding to 6.1 Wh/kg and 3.9 Kw/kg.

Future Directions

- Develop processes to improve cell producibility.
- Determine formulation to improve the initial performance and decrease performance fading.
- Develop hardware (aluminum case and connection) to reduce weight and cell impedance.

The purpose of this program is to develop electrochemical capacitors meeting DOE requirements. Consequently, this effort focuses on material evaluation and the cell fabrication processes. The down selection identified polyvinyl alcohol as the optimum binder from an evaluation of cells made of Norit SX Ultra as activated carbon. In this study it was found that manufacturing issues were critical. Coating formulation and processes were evaluated systematically. This resulted in establishing a producible process procedure, and adjustments of these processes were required when high-performance mesocarbon (very high surface area) was tried.

By the end of 1996, several cells made of 100% Maxsorb as active material were successfully manufactured and tested. Capacitance of more than 140 F capacitance and 20 mΩ resistance were obtained, which correspond to a total specific energy of 6.1 Wh/kg and a peak specific power of 3.9 kw/kg at 2.9 V. A total of 10 supercapacitor cells were delivered to Idaho National Energy Laboratory (INEL) for evaluation

III. APPLIED SCIENCE RESEARCH

The objectives of this program element are to provide and establish scientific and engineering principles applicable to batteries and electrochemical systems; and to identify, characterize and improve materials and components for use in batteries and electrochemical systems. Projects in this element provide research that supports a wide range of battery systems based on solid electrolytes and nonaqueous electrolytes, both liquid and polymer. Other projects are directed at research on improving the understanding of electrochemical engineering principles, corrosion of battery components, surface analysis of electrodes, and electrocatalysis.

A. ELECTRODE CHARACTERIZATION

Characterization of electrode morphology and chemical composition are important for the successful development of rechargeable electrodes for advanced secondary batteries. Efforts are underway to utilize advanced microfabrication techniques and spectroscopy to characterize electrode properties.

Carbon Electrochemistry

Kim Kinoshita
90-1142, Lawrence Berkeley National Laboratory, Berkeley CA 94720
(510) 486-7389, fax: (510) 486-4260

Objective

- Identify the critical parameters that control the reversible intercalation of Li into carbonaceous materials and determine their maximum capacity for Li intercalation.

Approach

- Couple electrochemical studies with physical measurements to correlate the relationship between the physicochemical properties of carbonaceous materials and their ability to intercalate Li.

Accomplishment

- A process involving catalytic chemical vapor deposition (CVD) has been developed to synthesize carbonaceous materials which have a reversible Li capacity of about 370 mAh/g.

Future Directions

- Characterize the properties of carbon by Raman spectroscopy and investigate the formation of the irreversible surface layer by ellipsometry.
- Continue *in situ* transmission electron microscopy (TEM) studies of lithiated carbons, and characterize the properties of heat-treated petroleum cokes for Li intercalation.

The objective of this project is to identify the critical parameters that control the reversible intercalation of Li in carbonaceous materials. This project involves investigations of the role of physicochemical properties of carbonaceous materials on their ability to reversibly intercalate Li. This latter effort is coordinated with the research conducted at LLNL to evaluate the intercalation of Li in carbonaceous materials for rechargeable Li batteries (see discussion in "Fabrication and Testing of Carbon Electrodes as Lithium Intercalation Anodes").

A process involving catalytic CVD has been developed to synthesize carbonaceous materials for use in Li-ion batteries. This process employs a transition metal catalyst in a tube reactor to produce the carbonaceous materials. The transition metal catalyst is used to improve the yield of carbon in the CVD process. A hydrocarbon precursor such as C_6H_6 or CH_4 is passed through a heated quartz tube (OD 18 mm) which contains a metal catalyst (*e.g.*, Ni or stainless steel) near the reactor-tube entrance. The hydrocarbon gas decomposes on the catalyst and forms a

carbonaceous deposit downstream in the tube which is heated to 500–1000°C. SEM analysis of carbon obtained by catalytic decomposition of methane showed that some fibers (~30-μm diameter) were formed. Samples of the carbonaceous materials were fabricated into electrode structures and investigated for Li storage capacity in 1.0 M $LiClO_4$ in propylene carbonate (PC). The reversible capacity of the carbon that was obtained by catalytic CVD of C_6H_6 is about 370 mAh/g, and a low irreversible capacity loss (30 mAh/g) was observed. Similar results were obtained with carbon produced by the catalytic CVD of CH_4 (380 mAh/g), except that the irreversible capacity loss (60 mAh/g) was greater.

The collaboration with Superior Graphite (Chicago IL) and LLNL continued with the focus to evaluate alternative graphitized carbons for the negative electrodes in Li-ion cells. The graphitized carbons obtained from Superior Graphite so far have demonstrated that high heat-treatment temperatures (~2800°C) may not be required to obtain acceptable electrode materials for Li-ion cells. To verify this observation and to evaluate another precursor material, additional samples were obtained from Superior Graphite. Electrochemical testing in 0.5 M $LiN(CF_3SO_2)_2$/ ethylene carbonate:dimethyl carbonate (EC:DMC) electrolyte and characterization by TEM are underway.

The irreversible capacity of lithiated carbons for negative electrodes in Li-ion batteries is strongly dependent on the type of electrolyte and physicochemical properties of the carbonaceous materials. Experiments involving ellipsometry and Raman spectroscopy were initiated to complement the present studies to understand the relationship between the properties of the carbon and the surface layer that is associated with the irreversible capacity loss. A preliminary design for an electrochemical cell that permits *in situ* ellipsometry to observe the formation of the surface layer on carbon has been completed. Initial experiments will utilize smooth carbon films that are formed by pyrolyzing a photo resist which is spin-coated onto a silicon wafer.

Raman spectroscopy, coupled with high-resolution transmission electron microscopy (HRTEM) and XRD analysis, were used to characterize the physical properties of carbonaceous materials obtained by heat treatment of petroleum coke at 1800, 2100 and 2350°C. The effects of heat treatment and air-milling process (to obtain an average particle size of 10 μm) on the physical and microstructural properties of the carbon particles were examined. The Raman intensities of the D and G bands were used to estimate the crystallite size L_a, and XRD was used to obtain L_c and the d(002) spacing of the petroleum cokes. Heat treatment of the petroleum coke at temperatures above 2100°C produces a L_a of about 100 Å, L_c of >600 Å, and d(002) spacing of 3.358 Å, close to that of graphite. HRTEM showed that a distinct ordering of the layer planes occurs with heat treatment, and a perceptible difference in the surface morphology is evident with petroleum coke that is heat treated at 2350°C and then air milled. The electrochemical results for Li intercalation/deintercalation of the petroleum cokes in 0.5 M $LiN(CF_3SO_2)_2$/EC:DMC electrolyte revealed that heat treatment at 2350°C improves the reversible Li storage capacity of the petroleum coke, and that air milling after heat treatment produces a petroleum coke with high reversible capacity, equivalent to $Li_{0.93}C_6$.

PUBLICATIONS

X.Y. Song, K. Kinoshita and T.D. Tran, "Microstructural Characterization of Lithiated Graphite," J. *Electrochem. Soc.*, **143**, L120 (1996).

K. Kinoshita, J. Bonevich, X. Song and T.D. Tran, "Transmission Electron Microscopy of Carbons for Lithium Intercalation," *Solid State Ionics*, **86-88**, 1343 (1996).

T.D. Tran, W.M. Goldberger, X.Y. Song and K. Kinoshita, "Lithium Intercalation in Heat-Treated Petroleum Cokes," in *Proceedings of the 8th International Meeting on Lithium Batteries*, June 16-21, 1996, Nagoya, Japan (1996) p. 105.

T.D. Tran, R.W. Pekala, W.M. Goldberger, X.Y. Song and K. Kinoshita, "Graphitized Needle Cokes and Natural Graphites for Lithium Intercalation," in *Proceedings of the Symposium on Microporous and Macroporous Materials*, J. Beck, L. Iton, D. Corbin, R. Lobo, M. Davis, S. Suib, S. Zones, eds., Materials Research Society, Pittsburgh, PA (1996).

E.J. Rudd, R. Putt, K. Kinoshita and X.Y. Song, "Oxygen Electrodes for Secondary Metal-Air Batteries," in *Proceedings of the Symposium on Oxygen Electrochemistry*, Vol. 95-26, R. Adzic, F. Anson and K. Kinoshita, eds., The Electrochemical Society, Inc., Pennington, NJ (1996) p. 189.

Fabrication and Testing of Carbon Electrodes as Lithium Intercalation Anodes

Tri D. Tran
L-365, Lawrence Livermore National Laboratory, P.O. Box 808, Livermore CA 94550
(510) 422-0915, fax: (510) 423-4897

Objectives

- Evaluate the performance of carbonaceous materials as hosts for Li intercalation negative electrodes.
- Develop reversible Li intercalation negative electrodes for advanced rechargeable Li cells.

Approach

- Fabricate electrodes from various commercial carbons and graphites and evaluate in small Li-ion cells.
- Correlate electrode performance (*i.e.*, capacity, irreversible capacity) with carbon structure and properties in collaboration with LBNL.

Accomplishments

- The Li intercalation capacities of petroleum needle cokes (190LS, Superior Graphite Co.) that were air milled and heat treated to 1800, 2100 or 2350°C were examined The highest Li intercalation capacity ($x = 0.93$ in Li_xC_6) was obtained with the sample that was heat treated at 2350°C and then air milled.
- Graphitized cokes from Superior Graphite exhibited reversible capacities of about 230 mAh/g (x near 0.62), comparable to that obtained with petroleum cokes from other sources.

Future Direction

- Continue evaluation of commercial and chemically modified carbon materials for Li intercalation.

A number of important factors which were expected to affect the performance of carbon and graphite for Li intercalation were investigated. These include the effects of heat treatment, milling (either before or after heat treatment), binder type and concentration, compression and current collector type. The results from these studies and related properties obtained from characterization experiments are discussed below.

Processing conditions such as milling (grinding) to pulverize the coarser particles can alter the particle surface morphology. In this work, we studied the effects of both heat treatment and milling (either prior to or after the heat treatment) to examine the relative significance of these two parameters on the intercalating ability of needle petroleum coke. The performance of natural graphite particles which have similar physical properties is included for comparison.

The coke material is a calcined type (190LS, Superior Graphite). This readily graphitizable coke is referred to as a needle petroleum coke and is used commercially to make large graphite electrodes. This particular coke material is low in sulfur (<1%) and other elements (0.050.15%). The cokes were processed according to the following procedures using identical time-temperature schedules: 1) the coarse grains (-3/8" mesh ROK) were heat treated and subsequently air milled to a fine powder (average particle size ~10 μm); 2) the coarse materials were air milled prior to heat treatment. The graphitization experiments were done in a laboratory graphite resistance tube furnace at three temperatures 1800, 2100, and 2350°C in a flowing argon stream. A sample designation 1800 M means that the coke was first treated to 1800°C before being milled (M) to the final size. The electrodes were prepared using a commercial, 0.12-mm thick carbon fiber sheet (Lydall Corp., Manchester, MA) as the support matrix and a carbonized phenolic resin binder (10-15%). Lithium foils (Cyprus Foote Mineral, Kings Mountain, NC) were used as the counter and reference electrodes. Fiberglass filters (Whatman 934-AH) were used as the separators between the working and counter electrodes. The electrolyte

was 0.5 M lithium (bis)trifluoromethanesulfonimide (HQ115, 3M Corp., St. Paul, MN) in 50:50 EC:DMC (Grant Chemical, Elmwood Park, NJ). The electrochemical experiments were carried out in a 15-ml, three-electrode cylindrical cell. Brunauer Emmett Teller (BET) BET surface area measurements were obtained with a multi-point method using a Micromeritics ASAP 2000 Surface Area Analyzer. Particle size distribution was available from Superior Graphite Co.

The physical properties and electrochemical intercalating parameters of the cokes and graphite are summarized in Table 2. The particle size distributions show a distribution with an average particle size near 10 μm. A higher maximum was observed with the samples that are milled after heat treatment. Nitrogen gas adsorption analysis showed a clear difference in the BET surface areas of the two sets of materials. The surface areas of samples that are milled after heat treatment are approximately twice as large as those milled before heating (Table 2).

The potential profiles of samples heat treated at temperatures below 2100°C show a sloping curve over the capacity range characteristic of behavior for amorphous carbons (Figs. 5 and 6), regardless of milling order. Flat plateaus below 0.25 V start to develop for materials processed at higher temperatures, indicating the development of ordered graphene layers associated with the graphitic structure. The trend here is in agreement with those reported for pitch cokes.

The Li capacity *vs.* heat treatment temperature curves for the two series of cokes show a minimum capacity (x = 0.45) at ~1800°C (Fig. 7). Additional data points are needed to clearly establish the minimum but the presence of one is evident. The series of electrodes made from materials milled after graphitization showed 15-20% higher capacities compared to those that were milled prior to heat treatment. Furthermore, the electrochemical behavior of sample 2350 M is remarkably similar to that observed for highly graphitic natural graphite (Table 2). Heat treatment conditions in this case apparently are sufficient for the highly graphitic crystalline structure to form. The sample microstructure will be examined in more detail by electron microscopy and XRD study. The irreversible capacity loss (Table 2) associated with the formation of the solid-electrolyte interphase does not appear to correspond with the BET surface areas as might be expected from the earlier studies.

The milling process represents more than a three order-of-magnitude change in the particle dimensions on a volumetric basis. As expected the materials milled after graphitization (1800, 2100 and 2350 M) contain an open structure with a large fraction of active edge-oriented surfaces to more fully utilize the bulk structure for insertion. On the other hand, graphitization of the milled powders could close off certain crystallites in the bulk structure which would not be accessible for insertion even at a slow rate (e.g., C/24). These results appear to be consistent with TEM observations.

Table 2. Physical properties and performance of treated cokes and a natural graphite

Sample	Process conditions	Particle size (μm)	BET area (m^2/g)	Capacity (x in Li_xC_6)	Irreversible capacity (mAh/g)
SO22	control, as-received	30-40	0.4	0.69	65
SO23	milling + 1800°C	10	5.6	0.45	81
SO24	milling + 2100°C	10	4.6	0.74	110
SO25	milling + 2350°C	10	4.3	0.81	130
SO26	1800°C + milling	10	9.3	0.56	72
SO27	2100°C + milling	10	9.8	0.82	70
SO28	2350°C + milling	10	9.2	0.93	69
BG74A	natural graphite	10	10	0.92	94

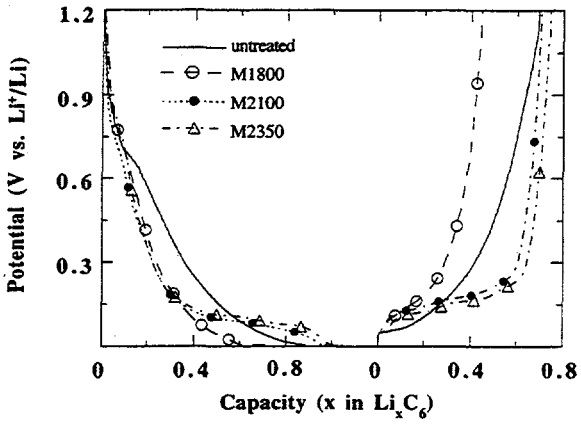

Figure 5. Discharge and charge potential profiles as a function of capacity of the initial petroleum coke and samples that were heat treated at 1800, 2100 and 2350°C after being air-milled.

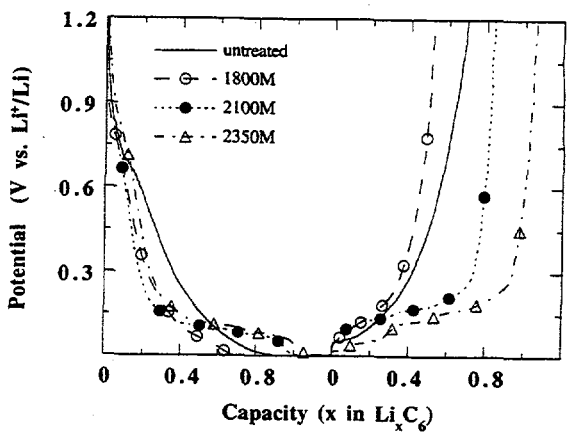

Figure 6. Discharge and charge potential profiles as a function of capacity of the initial petroleum coke and samples that were heat treated at 1800, 2100 and 2350°C before being air-milled.

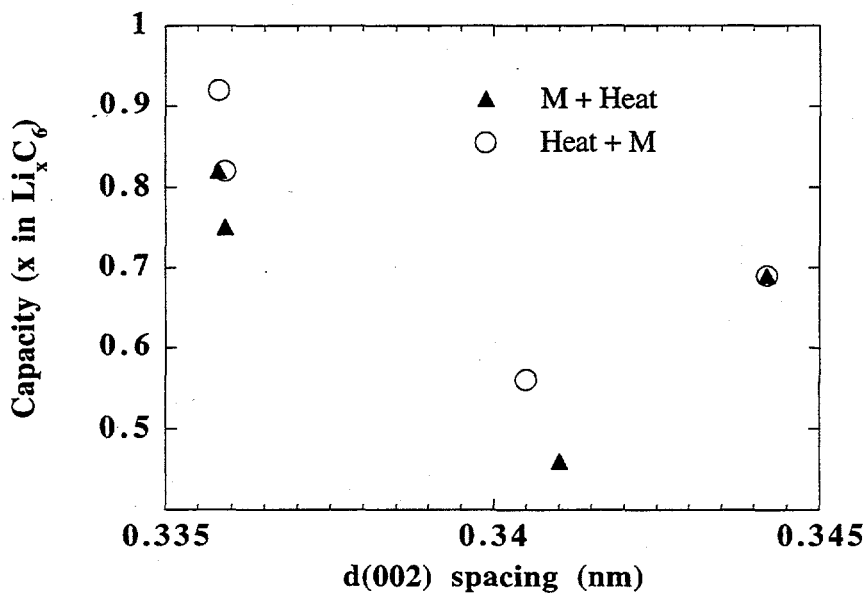

Figure 7. Change in Li storage capacity of petroleum cokes with processing conditions.

Battery Materials: Structure and Characterization

James McBreen
Brookhaven National Laboratory, DAS-Bldg. 480, P.O. Box 5000, Upton NY 11973-5000
(516) 344-4513, fax: (516) 344-4071

Objective

- Elucidate the molecular aspects of battery materials and processes by *in situ* synchrotron X-ray techniques.

Approach

- Apply *in situ* extended X-ray absorption fine structure (EXAFS) studies to obtain chemical information on zincate electrolytes.
- Apply EXAFS to the study of Li_xCoO_2, Li_xNiO_2 and $Li_xMn_2O_4$ electrodes.

Accomplishments

- New hermetically sealed spectroelectrochemical cells were developed for *in situ* XRD and X-ray absorption spectroscopy (XAS) studies of battery electrodes in rechargeable Li cells.
- By using high-energy X-rays (24.5 keV) it was possible to conduct *in situ* XRD on $LiMn_2O_4$ electrodes in unmodified commercial cells.
- EXAFS shows that complete removal of Li from Li_xNiO_2 eliminates the long-range order in the crystal.

Future Directions

- Continue *in situ* XRD and XAS studies of the cycling behavior and failure mechanisms of Li intercalation electrodes.
- Continue *in situ* high-resolution XRD and XAS studies of metal oxide Li intercalation electrodes with two transition elements.

The objective of this research is to elucidate the molecular aspects of materials and electrode processes in batteries and to use this information to develop electrode and electrolyte structures with good performance and long life. Work during the year included both *in situ* high-resolution XRD and EXAFS studies on cathodes for Li batteries.

***In Situ* High Resolution XRD Studies of $LiMn_2O_4$ Cathodes.** *In situ* XRD studies of cathode materials, using conventional X-ray sources are complicated because of the use of beryllium windows. When provisions are made to prevent corrosion of the beryllium the cell design is often quite different from that found in an actual battery. During the year techniques were developed to apply high-energy synchrotron X-rays (24.75 keV) for XRD studies in the transmission mode in commercial Li-ion cells with $LiMn_2O_4$ cathodes. These cells were encapsulated in plastic-aluminum laminates.

The XRD results indicate that $LiMn_2O_4$ is a highly irreproducible material. Some materials have secondary phases, which results in a region of two-phase coexistence on the first charge, at between approximately 60 to 80% of charge. The better-behaved materials exhibit only a single phase that contracts continuously in a single phase as Li is removed from the lattice during charge. The secondary phases in $LiMn_2O_4$ could not be detected with a conventional X-ray diffractometer. Even with the synchrotron X-rays it has been impossible to identify the material because only a few extra weak peaks were observed close to the peaks for the main cubic $LiMn_2O_4$ phase.

***In Situ* XAS Studies of $Li_xMn_2O_4$ and $LiNiO_2$ Electrodes.** New cells were designed for *in situ* XRD and XAS studies on both $LiNiO_2$ and $LiMn_2O_4$. These hermetically sealed cells were designed to be suitable for both *in situ* XRD and XAS studies of cathode materials for Li batteries in the transmission mode. The spectroelectrochemical cells are suitable for *in situ* studies of Li, Li-ion and Li-polymer-electrolyte cells at various temperatures up to 120°C.

Polytetrafluoroethylene-bonded (PTFE) $LiNiO_2$ cathodes were made using a roll-bonding technique and were incorporated into the cells with a Li foil negative electrode, a Celgard separator,

and a 1 M $LiPF_6$ electrolyte with a 1:1:3 PC:EC:DMC solvent. Considerable development work was necessary to fabricate cells that yielded both good electrochemical performance and XAS spectra. Figures 8 and 9 show typical spectra for a $Li/LiNiO_2$ cell at various stages of charge. The X-ray absorption near edge (XANES) spectra (Fig. 8) show a shift in edge energy to higher energies as the Ni oxidation state increases as Li is removed during charge. The Fourier transform of the EXAFS (Fig. 9) shows that midway through the charge there is considerable disorder in the Li_xNiO_2 material. Surprisingly, it reverts to a more-ordered structure towards the end of charge.

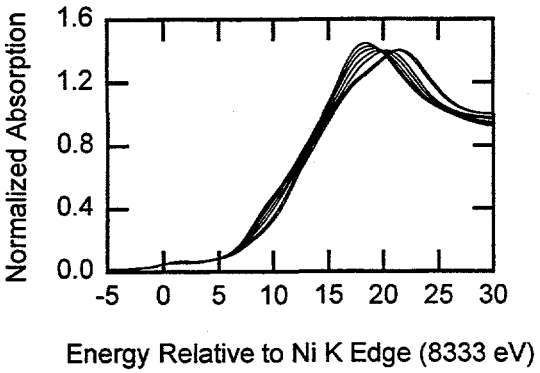

Figure 8. *In situ* Ni XANES for a Li_xNiO_2 electrode during charge; x = 1.0, 0.88, 0.77, 0.66, 0.54, 0.18 and 0.01.

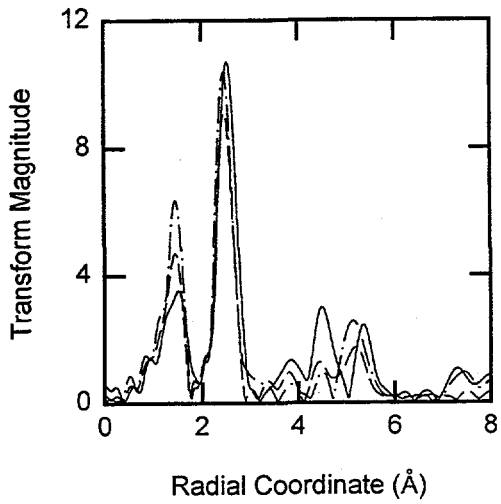

Figure 9. Fourier transform of Ni EXAFS for Li_xNiO_2 during charge; x = 1.0 (———), 0.54 (– – –) and 0.01 (– · — · –).

$LiMn_2O_4$ from E. Merck (Darmstadt, Germany) was used in cells with a 1 M $LiPF_6$ electrolyte in a 1:1:3 PC:EC:DMC solvent. Figures 10 and 11 show how the XANES and the Fourier transform of the EXAFS changes throughout the first charge. There are fewer changes in the spinel structure during charge than there are in the case of $LiNiO_2$. The feasibility of using cells of the same design to do *in situ* X-ray diffraction at the National Synchrotron Light Source (NSLS) in the transmission mode was demonstrated for both $LiNiO_2$ and $LiMn_2O_4$.

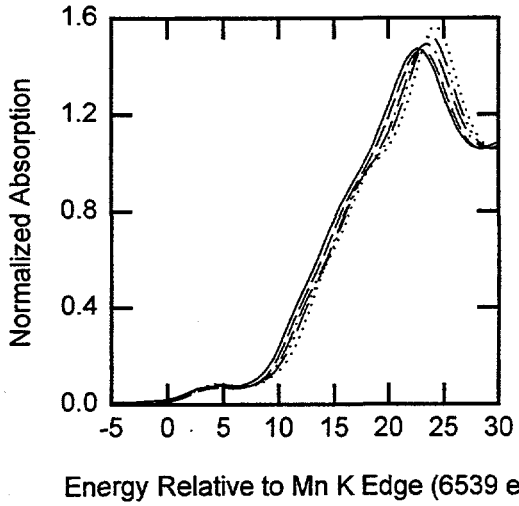

Figure 10. *In situ* Mn XANES for a $Li_xMn_2O_4$ electrode during charge; x = 1.0 (———), 0.75 (– – –), 0.5 (– · –), 0.75 (– ·· –) and 0.0 (····).

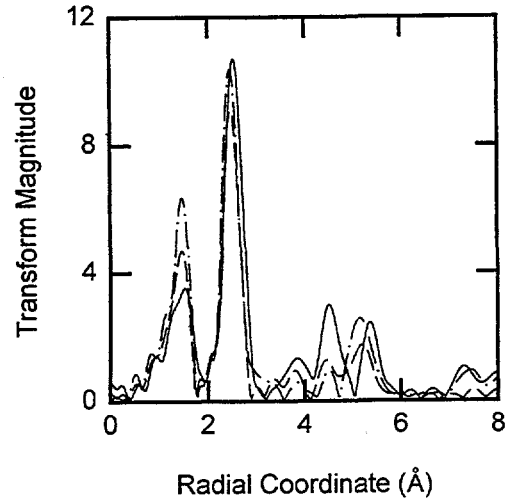

Figure 11. Fourier transform of Mn EXAFS for $Li_xMn_2O_4$ during charge; x = 1.0 (———), 0.50 (– – –) and 0.01 (– · — · –).

B. ELECTRODES FOR ELECTROCHEMICAL CELLS

Electrodes are being developed to identify low-cost metal hydrides for MH/NiOOH cells and improved metal oxides for electrochemical capacitors

Preparation of Improved, Low-Cost Metal Hydride Electrodes for Automotive Applications

James J. Reilly
Department of Applied Science, Bldg. 815, Brookhaven National Laboratory, Upton NY 11973
(516) 344-4502, fax: (516) 344-3137

Objectives

- Increase the energy density of metal hydride electrodes by preparing improved AB_5 and AB_2 electrodes.
- Develop an improved mathematical model for the electrochemical behavior of the MH_x electrode.

Approach

- Determine thermodynamic properties of alloy hydrides used in electrodes.
- Fabricate and test hydride electrodes.
- Apply XAS methods to determine the electronic structure, the local atomic environment and corrosion of alloy hydride electrode materials.

Accomplishments

- The composition and function of Co, Al and Mn were determined for a series of $La(Ni,Co,Mn,Al)_5$ alloys.
- It was demonstrated that the presence of Co and Al in AB_5 hydride electrodes strongly inhibits corrosion by reducing the lattice expansion and contraction in the electrochemical charge-discharge process and in the case of Co, by the formation of a corrosion-resistant surface layer.

Future Directions

- Determine the function of individual metal components in complex alloy hydride electrodes.
- Increase electrode storage capacity and lifetime, and decrease costs.
- Determine the structure and atomic environment of promising alloys to provide a rational basis for further improvement.

Metal hydride electrodes are an attractive substitute for the cadmium electrode in Cd/Ni batteries as they have a relatively benign environmental impact and higher energy densities. However, even though MH_x/Ni batteries are currently competitive in certain high-end applications, their potential as inexpensive, reliable, energy storage devices for automotive applications is far from realized: a severe penalty has been incurred in storage capacity and materials costs in order to inhibit corrosion and attain acceptable electrode cycle life. This is a serious problem which this program addresses. Thus, the major goals of this effort are to improve the specific energy of the metal hydride electrode, decrease corrosion, increase electrode cycle life, and decrease materials costs. In pursuit of these goals, a variety of types of alloy hydrides (particularly AB_5 and AB_2 materials) is studied with respect to their thermodynamic, electrochemical and surface properties as well as their bulk crystal structure. Other goals are extension of the operating temperature of MH_x/Ni batteries, the development of a mathematical model for the MH_x electrode, the determination and improvement of low-temperature discharge kinetics, and the improvement or replacement of the NiOOH electrode. The pursuit of these objectives involves the use of various tools and techniques including the development of *in situ* and *ex situ* XAS methods at the NSLS.

Function and Composition of AB_5 Electrodes. Deterioration of electrode performance due to corrosion of electrode components is a critical problem. The susceptibility of MH_x electrodes to corrosion is essentially determined by two factors, surface passivation due to the presence of surface oxides or hydroxides and the molar volume of hydrogen, V_H, in the hydride phase. V_H is important since it governs alloy expansion and contraction during the charge-discharge cycle. Large volume changes increase the flushing action of the electrolyte through the pores and microcracks of the electrode during each charge and discharge cycle thereby increasing the rate of contact of the alloy surface with fresh electrolyte and, consequently, the corrosion rate. Thus, when examining the effect of various substituents upon electrode corrosion the question always arises whether an observed change is due to a change in lattice expansion or to a change in surface passivation, *e.g.*, the formation of a corrosion-resistant oxide layer.

While the partial substitution of Ni by other metals has ameliorated the corrosion problem it has also resulted in high alloy costs (because of the incorporation of Co) and reduced storage capacity; *e.g.*, none of the substituted multicomponent hydrides approach the storage capacity of $LaNi_5H_6$. Thus, although the cycle life of substituted AB_5 electrodes is greatly extended over that of $LaNi_5$ a severe penalty in storage capacity is exacted for this improvement. Thus, with a view towards increasing storage capacity, cycle life and decreasing costs, the differential effects of Ni substitution by Co, Mn and Al in alloys having the generic composition of $La(NiCoMnAl)_5$ was investigated during the past year.

To elucidate the relationship between corrosion rate and composition it is necessary to quantitatively determine lattice expansion. This requires the determination of the atomic volume of H, V_H, in the respective metal hydride phase. V_H values for a number of pertinent alloys are listed in Table 3.

Effect of Co substitution. Cobalt is invariably present in commercial MH_x battery electrodes. It tends to increase hydride thermodynamic stability and inhibit corrosion. However, it is also expensive and substantially increases battery costs; thus, the substitution of Co by a lower-cost metal is desirable.

The cycle life of each of a series of electrodes of composition $LaNi_{4.3-x}Co_xMn_{0.4}Al_{0.3}$, (x = 0.0, 0.2, 0.4, 0.75) was determined. From these data the following parameters were calculated: $\%\Delta V/V$ where V is the volume of the alloy unit cell and ΔV is the increase in cell volume upon hydriding, hydrogen content (n), and the corrosion rate. $\%\Delta V/V$ and the corrosion rate are plotted *vs.* Co content in Fig. 12.

Table 3. V_H values for selected alloys.

Composition	V_H Å^3
$NdNi_{3.55}Co_{0.75}Mn_{0.4}Al_{0.3}$	2.66
$La_{0.25}Nd_{0.75}Ni_{3.55}Co_{0.75}Mn_{0.4}Al_{0.3}$	2.74
$LaNi_{3.55}Co_{0.75}Mn_{0.4}Al_{0.3}$	2.93
$La_{0.65}Pr_{0.35}Ni_{3.55}Co_{0.75}Mn_{0.4}Al_{0.3}$	2.97
$LaNi_{3.5}Co_{0.75}Mn_{0.4}Al_{0.3}$	3.00
$Mm_{0.3}Mm^*_{0.7}Ni_{3.55}Co_{0.75}Mn_{0.4}Al_{0.3}$	3.00
$LaNi_{3.95}Co_{0.75}Al_{0.3}$	3.02
$MmNi_{3.55}Co_{0.75}Mn_{0.4}Al_{0.3}$ Ce free	3.05
$LaNi_{3.55}Co_{0.75}Mn_{0.4}Al_{0.3}$	3.06
$La_{0.5}Nd_{0.5}Ni_{3.55}Co_{0.75}Mn_{0.4}Al_{0.3}$	3.07
$LaNi_{3.55}Co_{0.75}Mn_{0.4}Al_{0.3}$	3.07
$LaNi_{4.1}Co_{0.2}Mn_{0.4}Al_{0.3}$	3.09
$LaNi_{3.9}Co_{0.4}Mn_{0.4}Al_{0.3}$	3.09
$MmNiNi_{3.55}Co_{0.75}Mn_{0.4}Al_{0.3}$ [a]	3.10
$MmNi\ Ni_{3.55}Co_{0.75}Mn_{0.4}Al_{0.3}$	3.13
$La_{0.25}Ce_{0.75}Ni_{3.55}Co_{0.75}Mn_{0.4}Al_{0.3}$	3.15
$La_{0.5}Ce_{0.5}Ni_{3.55}Co_{0.75}Mn_{0.4}Al_{0.3}$	3.15
$La_{0.65}Nd_{0.35}Ni_{3.55}Co_{0.75}Mn_{0.4}Al_{0.3}$	3.15
$LaNi_{3.55}Co_{0.75}Mn_{0.14}Al_{0.3}$	3.16
$LaNi_{3.85}Co_{0.75}Mn_{0.38}$	3.20
$La_{0.8}Ce_{0.2}Ni_{3.55}Co_{0.75}Mn_{0.4}Al_{0.3}$	3.21
$MmNi_{3.5}Co_{0.75}Mn_{0.4}Al_{0.3}$	3.23
$LaNi_{4.3}Mn_{0.4}Al_{0.3}$	3.26
$La_{0.65}Ce_{0.35}Ni_{3.55}Co_{0.75}Mn_{0.4}Al_{0.3}$	3.24
$LaNi_{3.85}Co_{0.75}Mn_{0.04}$	3.35
$LaNi_{4.7}Al_{0.3}$	3.47
$MmNi_{4.3}Mn_{0.4}Al_{0.3}$	3.51

[a] Synthetic mischmetal *i.e.*, $La_{0.26}Ce_{0.52}Pr_{0.06}Nd_{0.16}$

The correlation between expansion and corrosion is rather weak; *e.g.*, even though the H content increases at x = 0.2-0.4 corrosion is decreased while expansion is unchanged. It is thus likely that corrosion inhibition by Co may also be due to a surface effect as with cerium. Recent XAS results also suggest that Co inhibits corrosion *via* a surface process by suppressing Ni oxidation as noted below.

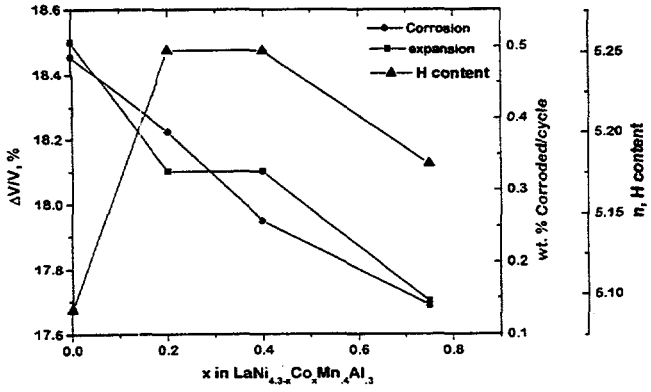

Figure 12. % ΔV/V, wt% corroded/cycle, and H content *vs.* Co content, x, in $LaNi_{4.3-x}Co_xMn_{0.4}Al_{0.3}$ electrodes.

Effect of aluminum. Cycle life experiments were carried for a homologous series of alloy electrodes of composition $LaNi_{3.85-x}Co_{0.75}Mn_{0.4}Al_x$ (x = 0,0.1, 0.2 0.3). The same experimental protocol was used as described above for Co. The corrosion-inhibiting effect of Al is clearly shown in Fig. 13. The presence of even a small amount of Al substantially decreases V_H, n and, consequently, both lattice expansion and corrosion.

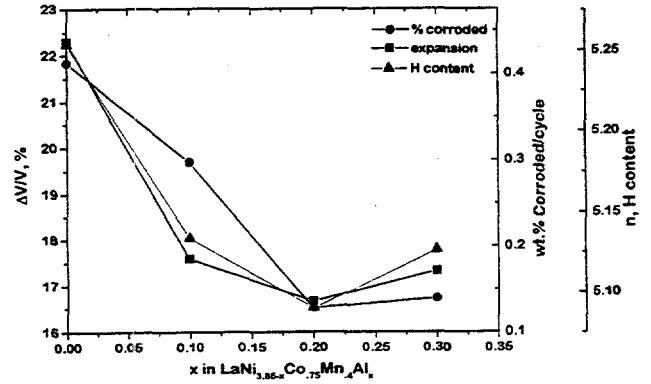

Figure 13. % ΔV/V, wt% corroded/cycle, and H content *vs.* Al content, x, in $LaNi_{3.85-x}Co_{0.75}Mn_{0.4}Al_x$ electrodes.

Effect of manganese. Again using the same experimental protocol the effect of Mn content was determined. The results are plotted in Fig. 14. The function of Mn is still open to question. It apparently increases V_H (Table 3) slightly and although the correlation between lattice expansion, n, and corrosion rate is fairly strong they are not functions of Mn content.

XAS Studies of AB_5 Hydride Electrode Materials. In support of the cycle life studies

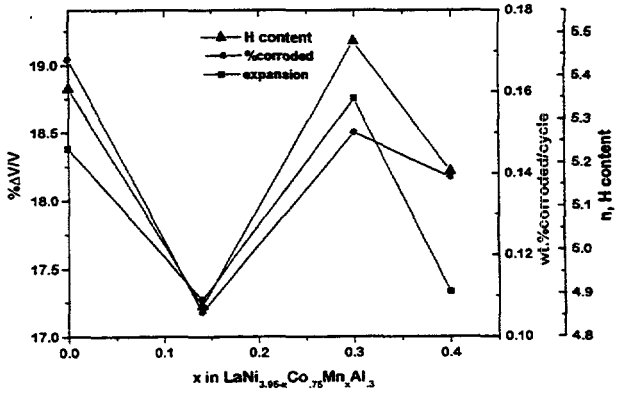

Figure 14. % ΔV/V, wt% corroded/cycle, and H content *vs.* Mn content, x, in $LaNi_{3.95-x}Co_{0.75}Mn_xAl_{.3}$ electrodes.

described above, XANES was used to further elucidate the role of Co in corrosion resistance. Similar studies were also carried out on Ce-substituted AB_5 electrodes with the object of comparing the previously reported corrosion inhibition by Ce with that of Co.

A total of three samples was examined: sample 1, $LaNi_{3.55}Co_{0.75}Mn_{0.4}Al_{0.3}$ (LaB_5); sample 2, $LaNi_{4.3}Mn_{0.4}Al_{0.3}$; sample 3, $La0.8Ce_{0.2}Ni_{3.55}Co_{0.75}Mn_{0.4}Al_{0.3}$ ($La_{0.8}Ce_{0.2}B_5$). In all cases the samples were previously activated and had an initial particle size of 2-4 μm as determined by BET measurements. In Fig. 15 the Ni K edge spectra are compared for samples 1 and 2 and show both bulk (transmission) and surface (electron yield) spectra after 100 charge/discharge cycles. The surface spectra represent the response from the particle surface to a depth of 20-30 nm. Comparison of the Ni K edge white lines in Fig. 15 clearly shows that the amount of Ni corrosion is directly related Co content. The electron yield spectra also show significantly higher surface segregation of Ni in the absence of Co. Conversely similar spectra at the Co K-edge for the $LaNi_{3.55}Co_{0.75}Mn_{0.4}Al_{0.3}$ show that a significant amount of Co segregates to the surface after 100 cycles (Fig. 16). These spectra further confirm the disintegration of alloy lattice structure close to the surface as a result of cycling.

The corrosion-inhibiting effect of Ce was confirmed using the same XANES technique. This is shown in Figs. 17 and 18 for $La_{0.8}Ce_{.2}B_5$ which shows greatly reduced concentrations of oxidized Ni and Co on the alloy surface relative to LaB_5. It is known that Ce has the ability to form a protective oxide on metal surfaces and a similar mechanism may be operating in this instance.

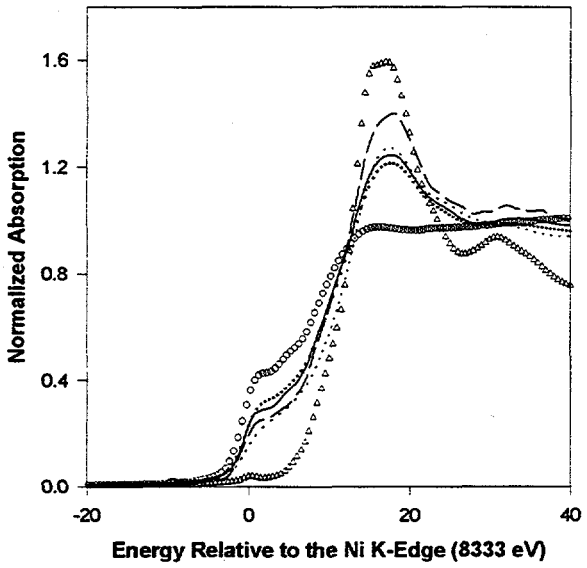

Figure 15. Ni K-edge XANES spectra for $LaNi_{3.55}Co_{0.75}Mn_{0.4}Al_{0.3}$ (Transmission [+], E-yield [...]) and $LaNi_{4.3}Mn_{0.4}Al_{0.3}$ (Transmission [—], E-yield [– – –]) showing the corrosion of Ni after cycling 100 times relative to an uncycled LaB_5 electrode (O) and pure β $Ni(OH)_2$ (Δ). The results show that partial substitution of B component by Co reduces the amount of Ni corrosion on the alloy surface products.

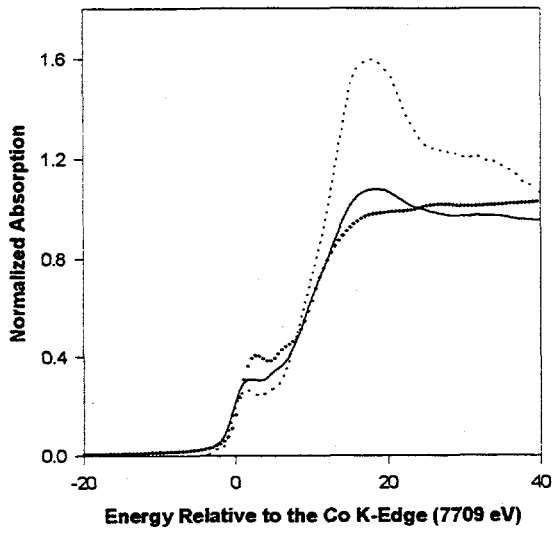

Figure 16. Co K-edge XANES spectra for LaB_5 (Bulk [—], Surface [...]) after 100 cycles *vs.* an uncycled electrode (+). The large white line indicates buildup of $Co(OH)_2$ on the alloy surface.

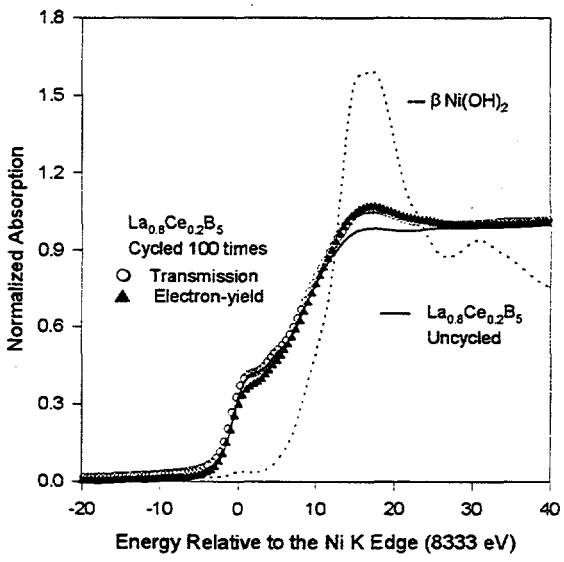

Figure 17. Ni K-edge XANES spectra for $La_{0.8}Ce_{0.2}B_5$ (Bulk [O], Surface [▲]) showing the corrosion of Ni after cycling relative to an uncycled electrode (–) and pure β–$Ni(OH)_2$ (...). The results show that partial substitution of the A component by Ce reduces the amount of Ni corrosion on the alloy surface products.

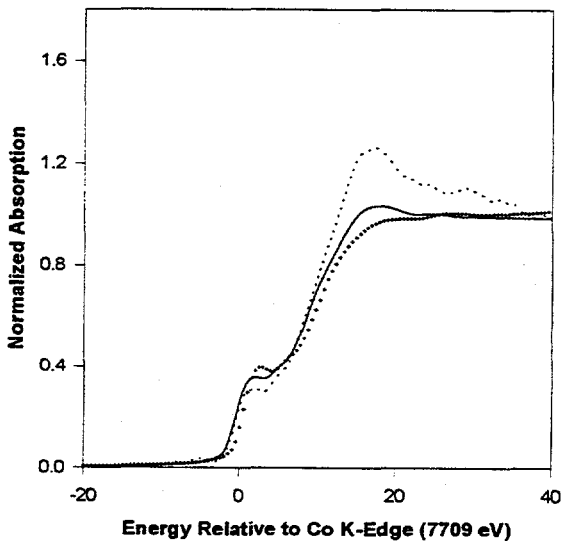

Figure 18. Co K-edge XANES spectra for $La_{0.8}Ce_{0.2}B_5$ (Bulk[—], Surface[...]) after 100 cycles *vs.* an uncycled electrode (+). The large white line indicates buildup of $Co(OH)_2$ on the alloy surface.

Optimization of Metal Hydride Properties in MH/NiOOH Cells for Electric Vehicle Applications

Ralph E. White
Department of Chemical Engineering, University of South Carolina, Columbia, SC 29208
(803) 777-7314, fax: 803)777-8265

Objectives

- Optimize the alloy composition of metal hydride electrodes by microencapsulation of hydrogen-storage alloys.
- Determine the exchange current density, diffusion coefficient, symmetry factor and equilibrium potential of bare and Cu-coated $LaNi_{4.27}Sn_{0.24}$ electrodes as a function of the state of charge.
- Develop improved metal hydride electrodes for MH/NiOOH batteries..

Approach

- Prepare bare and Cu-coated $LaNi_{4.27}Sn_{0.24}$ electrodes for determination of transport and electrochemical kinetic parameters.
- Apply porous electrode theory to data obtained from the $LaNi_{4.27}Sn_{0.24}$ electrodes in alkaline solutions to determine kinetic parameters.
- Determine the diffusion coefficient of hydrogen in the hydride.

Accomplishments

- A mathematical model for a spherical metal hydride particle has been derived which can be used to predict the electrode potential at various discharge rates as a function of state of charge.
- The apparent activation enthalpy at different states of charge was determined by measuring the polarization resistance of electrodes at different temperatures. It was found that it is an indicator of the relative reaction rate of the charge-transfer reaction and of hydrogen absorption.
- Microencapsulation of the hydrogen storage alloys with electroless Ni or Co-Ni coatings was found to improve the cycle life by forming a conductive passive film on the surface which prevents the oxidation of the active materials.

Future Direction

- Determine the cycle life of bare and coated alloys as a function of temperature.

The objective of this project is to improve the cycle life of M-H electrodes by microencapsulating the alloy (*i.e.*, $LaNi_{4.27}Sn_{0.24}$) with thin layers of metals/alloy (Cu, Ni, Co, Co-Ni) by electroless deposition. Copper plating of the hydride particles was carried out in steps. The hydride surface was activated by immersing the powder in an aqueous HCl solution of $SnCl_2$, and then in an aqueous HCl solution of $PdCl_2$. Electroless Cu deposition was then carried out in alkaline electrolyte containing HCHO. The Cu-to-metal-hydride-alloy ratio was $^1/_4$ by weight, which yielded a thickness of the metallic Cu layer <1 μm. The process of electroless Cu plating was terminated when the deep blue color arising from the Cu complex vanished. Highly magnetic Co-Ni alloys were obtained. Good adhesion between the particles reduces the particle-particle contact resistance and also reduces the amount of binder to be added during the preparation of the alloy. The discharge curves of Co-plated and Co-alloy-plated M-H reveal two discharge plateaus. This behavior is unique to the Co-plated alloy and was not seen for Ni, Cu or Pd plated alloys. The potential drops drastically due to depletion of hydrogen at the surface and reaches a plateau again at approximately -0.7 V. The potential remains constant for a certain period of time and then drops to -0.6 V. An increase in the capacity of the electrode was seen and was attributed to the formation of cobalt hydroxide on the surface of the encapsulated alloy. The cobalt hydroxide formed

in the presence of additives in the electrolyte dramatically increases the cycling life of the electrode. Further studies are currently being done to elucidate the discharge mechanism of Co, Co-Ni and Co-Ni alloys and to determine their cycle life.

The effect of temperature on the performance of metal hydride electrodes was investigated in the temperature range of 0 to 50°C. The electrodes showed a maximum discharge capacity at 25°C. The total resistance increases with a decrease of temperature over the entire temperature range. The observed loss in capacity at low temperatures was due to the high internal resistance, while the loss observed at high temperatures was caused by the self discharge. The ohmic resistances and polarization resistance were determined from the electrochemical impedance spectroscopy (EIS) data by fitting an equivalent circuit.

A mathematical model was developed that can be used to predict the electrode potential at various discharge rates as a function of the state of charge. It could be seen that as the discharge rate increased the state of discharge at the end-of-discharge decreased. This behavior was explained by the depletion of atomic hydrogen on the surface of the M-H particles at high discharge rates, because of the hydrogen diffusion limitation in the bulk of the hydride. Thus for high discharge applications, alloys with high exchange current density are preferred. However, for a complete utilization of the electrode a low exchange current density is desirable.

PUBLICATIONS

B.N. Popov, G. Zheng and R.E. White, "Determination of Transport and Electrochemical Kinetic Parameters of M-H Electrodes," *J. Appl. Electrochem.*, **26**, 603 (1996).

G. Zheng, B.N. Popov and R.E. White, "Determination of Transport and Electrochemical Kinetic Parameters of Bare and Copper-Coated $LaNi_{4.27}Sn_{0.24}$ Electrodes in Alkaline Solution," *J. Electrochem. Soc.*, **143**, 834 (1996).

G. Zheng, B.N. Popov and R.E. White, "Application of Porous Theory on Metal Hydride Electrodes in Alkaline Solution," *J. Electrochem. Soc.*, **143**, 435 (1996).

Microstructural Modeling of Highly Porous MH/NiOOH Battery Substrates

Ann Marie Sastry
Department of Mechanical Engineering and Applied Mechanics, The University of Michigan, Ann Arbor, MI 48109-2125
(313) 764-3061, fax: (313) 747-3170

Objectives

- Develop predictive capability for determining performance of MH/NiOOH secondary cells through microstructural modeling of the NiOOH electrode.
- Improve the specific energy of MH/NiOOH batteries by determining optimal microstructures for NiOOH substrates.

Approach

- Develop closed-form approaches for efficient calculation of transport coefficients in porous fibrous microstructures.
- Develop standards for cell cycling which allow verification of closed-form models for electrode failure.
- Use microstructural descriptions of actual materials to initiate coupled stochastic/mechanical simulations of failure progression.

Accomplishments

- Materials were characterized microscopically and simulations of transport in model microstructures have been completed.
- A novel network-generation approach has been validated with experimental resistivities in fibrous substrates.
- A new mechanics technique has been developed to model the damage progression in the fibrous substrates, and damage simulations have been initiated.

Future Directions

- Expand interaction approach to accommodate all microstructures present in substrates.
- Conduct large-scale simulation of transport behavior in random networks and full-scale cell testing to assess accuracy of models.
- Develop new standards for cell testing to better assess electrode performance.

The objective of this program is to develop predictive capability of performance of MH/NiOOH secondary cells through microstructural modeling of electrode behavior. The study is focused on the effects of the microstructure of fibrous composite electrodes on thermal and electrical conductivity, strength, and lifetime. Several candidate materials have been acquired and studied. Electrode failures after multiple charge-discharge cycles are being modeled at the microstructural level, incorporating failure mechanisms of the constituent materials, *e.g.*, Ni fatigue and subsequent loss of conductivity. The theoretical approaches incorporate closed-form solutions for transport in electrode substrates with statistical, microstructural simulations.

Sample substrate materials, which vary in staple fiber length, connectivity of microstructure and porosity, were characterized optically. The materials under study are primarily comprised of sinter-bonded Ni fibers, some containing Ni spheroids, with porosities ranging from 80-95%, and with substantial variability in the samples. Software was acquired to perform detailed, digital micrographic analysis on these dry samples, and analytical techniques for interpretation of micrographic data were significantly refined.

Statistical distributions of all key features have now been identified (Fig. 19), and concurrent simulations in transport have used these distributions to test theoretical results (Fig. 20).

Both full-blown finite element techniques, and the novel reduced network approach have been used. The novel approach has been shown to be significantly less computationally intensive, and provide acceptable descriptions of substrate behavior. Current efforts have focused on the use of this approach to generate networks for study under conditions of progressive mechanical damage, and a new mechanics technique has been developed to model the progressive damage.

A schematic of the deformation of fibers is shown (Fig. 21).

A custom battery test system has been acquired, and programmed with all USABC standard test techniques. Currently, this system is running high-rate charge-discharge tests on tri-electrode MH/NiOOH cells with positive plates constructed from the fibrous substrates under study. These experiments are at constant current at C/3 rate; cutoff is at 80% utilization or ~40 cycles for subsequent evaluation of damaged positive plates. The active material was removed to expose the dry substrate in the tested positive plates to examine the damaged materials. Optical evaluation has been initiated, for use in benchmarking studies of the mechanical damage simulations, in conjunction with the transport analysis.

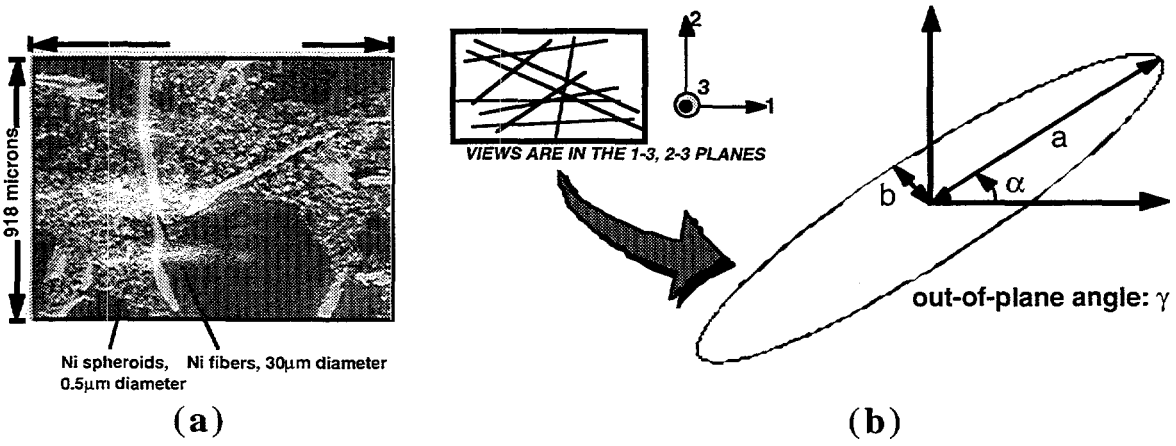

Figure 19. (a) Optical light micrograph of substrate material (National Standard Fibrex 50/50 Ni/Ni powder). (b) Image analysis showing key geometric features.

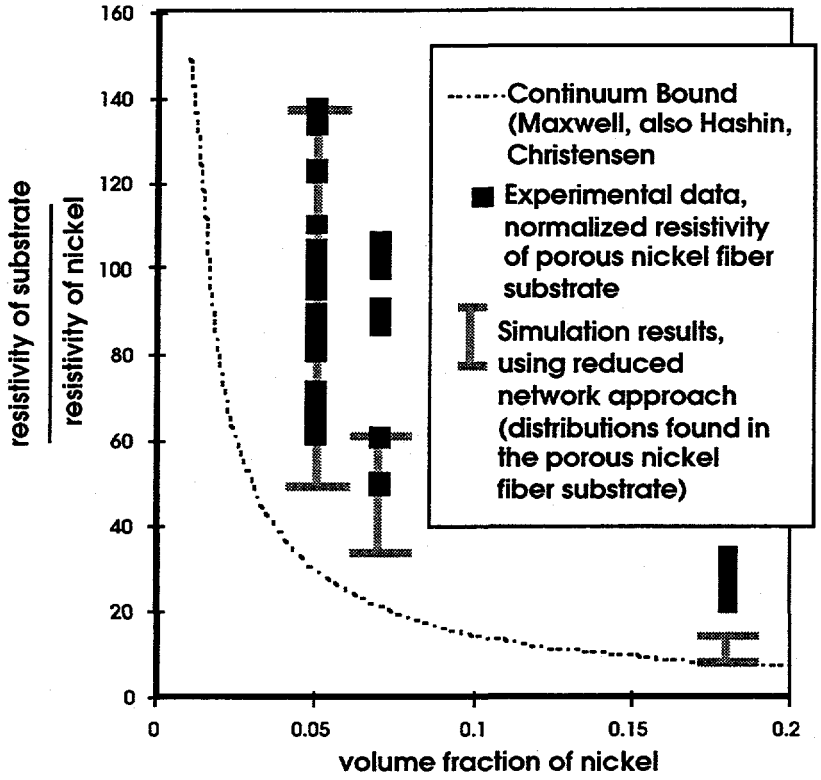

Figure 20. Experimental data, new approach and classic continuum approaches. Note the underestimate of resistivity (overly resistive materials short cells) of the continuum bounds. The new methods acceptably predict variability in resistivity in low volume fractions.

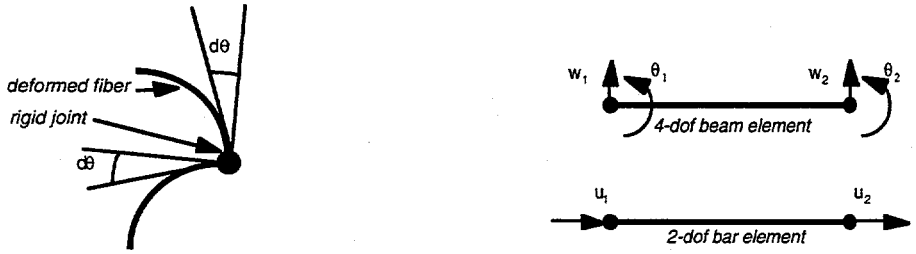

Figure 21. Network loading scheme. Point bonds are assumed rigid; segment geometry can be altered through moment of inertia and aspect ratio.

The elements shown are superposed to obtain the stiffness matrix, where [T] is the transformation matrix:

$$[K'] = \int_0^L [B]^T EI[B]dx = \frac{AE}{L}\begin{bmatrix} 1 & 0 & 0 & -1 & 0 & 0 \\ 0 & 0 & 0 & 0 & 0 & 0 \\ 0 & 0 & 0 & 0 & 0 & 0 \\ -1 & 0 & 0 & 1 & 0 & 0 \\ 0 & 0 & 0 & 0 & 0 & 0 \\ 0 & 0 & 0 & 0 & 0 & 0 \end{bmatrix} + \frac{EI}{L^3}\begin{bmatrix} 0 & 0 & 0 & 0 & 0 & 0 \\ 0 & 12 & 6L & 0 & -12 & 6L \\ 0 & 6L & 4L^2 & 0 & -6L & 2L^2 \\ 0 & 0 & 0 & 0 & 0 & 0 \\ 0 & -12 & -6L & 0 & 12 & -6L \\ 0 & 6L & 2L^2 & 0 & -6L & 4L^2 \end{bmatrix}$$

PRESENTATIONS

A.M. Sastry, X. Cheng, S.B. Choi and L. Huang, "Damage Analysis of Porous Structures," presented at the *American Society for Mechanical Engineers Winter Annual Meeting*, Computational Modeling of Damage in Composite Materials and Structures Symposium, Atlanta, GA, November 17-22, 1996.

A.M. Sastry, X. Cheng and S.B. Choi, "Transport in Porous Substrate Materials in Electrochemical Applications," presented at the *American Society for Mechanical Engineers Winter Annual Meeting*, Cellular and Microcellular Materials Symposium, Atlanta, GA, November 17-22, 1996.

A. M. Sastry, X. Cheng, S.B. Choi, L. Huang and N.V. Shah, "Microstructural Damage Analysis of Porous Substrate Materials," presented at the *Annual Technical Meeting of the Society for Engineering Sciences*, Tempe, AZ, October 20-23, 1996.

A.M. Sastry, X. Cheng, L. Huang, S.B. Choi and N.V. Shah, "Damage Evolution in Porous Fibrous Substrate Materials for Automotive NiMH Cells," *The 190th Meeting of The Electrochemical Society*, San Antonio, TX, October 6-11, 1996.

Sol-Gel Derived Metal Oxides for Electrochemical Capacitors

Marc A. Anderson
Water Chemistry Program, University of Wisconsin-Madison, 660 North Park Street, Madison, WI 53706
(608) 262-2470; fax: (608) 262-0454

Objectives

- Investigate the chemical and materials properties of the NiO/Ni system for electrochemical capacitors.
- Model and design metal oxide electrodes for improved electrochemical capacitors.

Approach

- Utilize sol-gel processing techniques to fabricate thin-film electrodes for electrochemical capacitors.

Accomplishments

- Prototype thin-film cells were successfully fabricated from nickel oxide thin-film electrodes.
- The specific energy, specific power and volumetric energy density (based on the active material) obtained from a nonaqueous thin-film cell were 11.85 Wh/kg, 1200 W/kg, and 16.9 Wh/liter, respectively.

Future Direction

- Complete evaluation of NiO/Ni electrodes in aqueous and nonaqueous electrolytes.

The specific capacitance of the nickel oxide electrode was investigated in various types of electrolytes. The highest specific capacitance of ca. 260 F/g was obtained in 1 M LiOH solution. The specific capacitance in 1 M KOH was ca. 160 F/g. A mixed electrolyte (0.5 M LiOH/0.5 M KCl) provided a specific capacitance of ca. 200 F/g. Two non-alkaline electrolytes (1 M KCl and 1 M LiCl) only provided specific capacitances of 5-10 F/g. It appears that these two electrolytes only store charge using the double-layer capacitance of the system, whereas the OH ligand is the main source of charge transfer processes (*i.e.*, pseudo-capacitance) in this nickel oxide system. Non-aqueous electrolytes can be employed with NiO-based capacitors. The high applied potentials of these electrolytes can enhance the energy density of this material system. The specific capacitance of a nickel oxide coated electrode in a common non-aqueous electrolyte, 1 M $LiClO_4$ in propylene carbonate, was ca. 26 F/g. At an applied potential of 4 V, the energy density of this system was ca. 72 J per gram of active material.

The charge-storage mechanism of the nickel oxide electrode can be described as

Aqueous Electrolyte (while charging):
Positive Electrode: $NiO+OH^- \longrightarrow NiOOH + e^-$
Negative Electrode: $NiOOH + e^- \longrightarrow NiO + OH^-$

Non-aqueous Electrolyte (that contains Li^+):
$Ni_xO + LiNiO_2 \longleftrightarrow Li_y\text{--}Ni_{x-\partial}O + Li_{1-y}Ni_{1+\partial}O_2$

Prototypes made from nickel oxide thin-film electrodes have been successfully fabricated using a thin-cell configuration. The total thickness of the cell (including outside packaging material) is less than 1 μm. Excluding the packaging materials, the thickness is only about 0.2 μm. Several combinations were tested, including a single cell with aqueous electrolyte, a single cell with nonaqueous electrolyte, and a three-stack cell with aqueous electrolyte. These tests proved the feasibility of employing nickel oxide as an active material for electrochemical capacitors. The capacitance values of these prototypes varied from 0.2 to 1 F or higher, depending on the manufacturing process. The cycle life of the cells was tested for 700 cycles with no loss in capacity. Because the ability to test cycle life was limited by the time available for testing and the test instruments, it is likely that the real life time of these units is much longer than 700 cycles. This material system appears to provide a flexible and cost-effective manufacturing route for building electrochemical capacitors that are characterized by high energy densities and power densities. The specific energy, specific power and volumetric energy density (based on only the active material) obtained from the single cell with nonaqueous electrolyte were 11.85 Wh/kg, 1200 W/kg, and 16.9 Wh/liter, respectively.

Several electrochemical techniques have been employed to demonstrate that the electrochemical reaction that occurs in this nickel oxide system is a surface redox reaction. This type of reaction results in fast charge transfer processes. Based on these results, it appears that other metal oxides might also be good candidates for use as active materials in electrochemical capacitors. Several metal oxides have been chosen for study as low-cost, environmental friendly materials in electrochemical capacitors.

PUBLICATIONS

K.-C. Liu and M.A. Anderson, "Ni_xO/Ni Composite Thin Films for Electrochemical Capacitors," in *Proceedings of the Symposium on Electrochemical Capacitors*, F.M. Delnick and M. Tomkiewicz, eds, PV95-29, The Electrochemical Society, Pennington, NJ (1996) p. 68.

K.-C. Liu and M.A. Anderson, "Evaluation of Current Collectors in Nickel Oxide Based Electrochemical Capacitors," in *Proceedings of the Symposium on Electrochemical Capacitors*, F.M. Delnick and M. Tomkiewicz, eds, PV95-29, The Electrochemical Society, Pennington, NJ (1996) p. 78.

C. COMPONENTS FOR AMBIENT-TEMPERATURE NONAQUEOUS CELLS

Metal/electrolyte combinations that improve the rechargeability of ambient-temperature, nonaqueous cells are under investigation.

Novel Lithium/Polymer-Electrolyte Cells

Elton J. Cairns and Frank R. McLarnon
90-1142 , Lawrence Berkeley National Laboratory, Berkeley CA 94720
(510) 486-4636, fax: (510) 486-4260

Objectives

- Investigate the behavior of electrodes in high-performance rechargeable batteries, and investigate means for improving their lifetime and performance.
- Improve the utilization of the sulfur electrode.
- Identify new electrode structures which will eliminate or minimize this fundamental mechanism of capacity loss of Li/MnO_2 cells.

Approach

- Fabricate and test Li/polymer electrolyte/sulfur cells.
- Use a completely new approach to synthesize a homogeneous "nano-scale" dispersion of a MnO_x entity inside a polymer matrix.

Accomplishments

- Greatly improved utilization of the sulfur active material in the range of 40% and higher was demonstrated.
- A novel aerogel $Li_xMn_yO_4$ powder with very high surface area was prepared with a sol-gel technique.

Future Directions

- Improve the utilization of the S electrode by reducing the size of the S particles in the electrodes.
- Optimize the performance of MnO_x including post-test characterization to identify the structure of the active component.

Li/S Cells. Earlier galvanostatic cycling of Li/polymer/S cells yielded poor active material utilization. In addition, unusual phenomena were observed, including discoloration of the polymer electrolyte surrounding the sulfur electrode and very long charge half-cycles with flat voltage plateaus. To address the cause(s) of these phenomena, different polymer and polymer gel electrolytes were tested, including amorphous polyethylene oxide (PEO). However, these changes did not significantly alter the cell characteristics stated above.

Following the July 1996 issuance of a U.S. patent to PolyPlus Battery Company (Berkeley, CA) for Li/polymer/S batteries, modifications were made to the composition and processing of electrodes and electrolyte in an effort to duplicate the high-capacity cell cycling claimed in this patent. Following a typical protocol, in which a salt-free PEO-based "electrolyte" is described, a sulfur electrode was produced with much less Li salt than previously used. In addition, dispersant was excluded from the electrode, and the electrodes were processed by casting directly onto the current collector, yielding thinner electrodes. We also used a more-structured, lower-density acetylene black which yielded better dispersions. These changes resulted in greatly improved utilization of the active material in the range of 40% and higher, but rapid capacity fade remains a problem. The electrolyte discoloration and extended charges persist, although with higher-rate cycling the latter effect is not always present.

Li/MnO_2 Cells. A novel aerogel $Li_XMn_yO_4$ powder with very high surface area was prepared with a sol-gel technique. Preliminary cell tests with this material showed good performance but poor stability. We are presently investigating the cause(s) of the poor stability, and formulating modifications to the preparation procedure.

PUBLICATIONS

W. Taucher, T.C. Adler, F.R. McLarnon and E.J. Cairns, "Development of Lightweight Nickel Electrodes for Zinc/Nickel Oxide Cells," *J. Power Sources* , **58,** 93 (1996).

Z. Deng, J.D. Spear, J.D. Rudnicki, F.R. McLarnon and E.J. Cairns, "Infrared Photothermal Deflection Spectroscopy: A New Probe for the Investigation of Electrochemical Interfaces," *J. Electrochem. Soc.*, **143,** 1514 (1996).

Polymer Electrolyte for Ambient Temperature Traction Batteries: Molecular Level Modeling for Conductivity Optimization

Mark A. Ratner
Department of Chemistry, Northwestern University, Evanston IL 60208-3133
(847) 491-5371, fax: (847) 491-7713

Objectives

- Analyze properties of polymer electrolytes by molecular dynamics and Monte Carlo simulations.
- Develop a microscopic understanding of the stability, structure and conduction properties of polymer electrolytes.
- Suggest modified materials with optimized conduction properties, based on mechanistic insight.

Approach

- Apply molecular dynamics and Monte Carlo simulations using high-speed computers to analyze the properties of polymer electrolytes

Accomplishments

- A general method for analysis of ion dynamics during energy-conversion cycles, including redox properties at the electrode/electrolyte interface was developed .
- MonteCarlo models for composite, polymer-based electrolyte structures were developed, and the investigation of optimized composite morphologies was begun.

Future Direction

- Analyze viscoelastic properties (hopping models) and transport (hopping/ dynamic percolation pictures) for composite electrolytes, based on inorganic fillers and polyelectrolyte hosts and compare with experimental results to deduce optimal filler structure and composition.

Previous modeling work has demonstrated that the simplest motif for polymer electrolytes (complexes between uni-univalent Li salts and neat polar polymers) will, like all dense fluid electrolytes, exhibit conduction maxima dominated by the relaxation properties of the polymer host. This not only implies a conductivity maximum of ~0.0001S/cm, but also a trade-off between the viscoelastic properties and conductance – a Walden-like relationship between them holds, so that the local microviscosities cannot be increased without cost to the conductance. Additionally, these simple polymer-salt-complex electrolytes have substantial disadvantages for battery applications: they can exhibit undesirable interfacial chemical reactivity with finely deposited Li, and they can lead to formation of dendrites, with resulting cell shorting and battery failure.

The two principal theoretical methods we have used are molecular dynamics, which gives a complete picture of the evolution of every particle (ion, solvent) in the system, and hopping dynamics, which follow only the ions themselves. We have shown conclusively that the hopping model will reproduce the important experimental properties (diffusivity, conductivity), and their temperature dependence. Molecular-dynamics simulations, which are more costly and more demanding, do yield additional information such as the vibrational spectrum and relaxation properties, but for our initial work on the complicated problem of composites, we will limit ourselves to the hopping methods. These are entirely appropriate, since they can take into account the most-important phenomena (percolation limitation by the filler particle mass, interfacial acceleration due to space-charge effects arising from the coulomb interaction, ion clustering and dynamics arising from evolution due to co-ions). To permit such computation, it is necessary to have the proper formulation theoretically – that is, it is necessary to deal with the boundary conditions created by the presence of both the filler particles and the coulomb interaction. An important and critical step in this area has been taken by an appropriate Green's function-based formulation of the boundary condition problem arising from the presence both of

coulomb interactions and of inaccessible regions for the ions. This work is highly mathematical and technical, but we feel that it represents an important advance, that permits actual calculation of the dynamics in coulomb systems with limited spatial homogeneity (precisely the situation for polymer-based composite electrolytes).

Essentially, one must solve simultaneously the Newton equations for particle motion (or, in the hopping model, the master equation for ion motion) and an equation determining the potential. The total potential can be written $V_{tot}(x) = V_c(x) + V_{hb}(x)$. Here the potential felt by an ion at position x is the sum of a coulomb interaction arising from the other charges, and a hard-body interaction arising from the presence of filler particles, in which ion mobility vanishes. The coulomb potentials, in turn, are the solutions to the Poisson equation. The long-range nature of the coulomb potential requires periodic boundary conditions (Ewald construction) for proper valuation of the forces acting on any given ion.

The constructions that we have developed from earlier work by Halley and collaborators, details the appropriate means for constructing the effective potential to do periodic images of the coulomb interaction, for situations in which the polymer-based material is inhomogeneous. This involves a generalization of the image rules used for simple absorption at metals. It provides a mathematically well-defined, computationally accessible means of computing the total coulomb potential in these systems.

We have begun coding the hopping model for inhomogeneous materials using this construct. These simulations will, we feel, be of substantive importance in understanding and optimizing the properties of composite materials, based on polymers, that are extremely promising for thin-film electrolytes in all-solid-state cells.

PUBLICATION

J.W. Perram and M.A. Ratner, "Simulations at Conducting Interfaces: Boundary Conditions for Electrodes and Electrolytes." *J. Chem. Phys.* **104**, 5174 (1996).

The Performance of New Materials for Polymer-Electrolyte Batteries

Duward F. Shriver
Department of Chemistry, Northwestern University, Evanston IL 60201-3133
(847) 491-5655, fax: (847) 491-7713

Objectives

- Synthesize polymer electrolytes based on aluminosilicate-polyether hybrid polyelectrolytes with improved low-temperature performance and higher cation transport number.
- Develop improved polymer electrolytes for rechargeable Li/polymer batteries.

Approach

- Synthesize polymer electrolytes to evaluate in electrochemical cells.

Accomplishment

- Polymer electrolytes based on $[PN(OCH_2CH_2OCH_2CH_2OCH_3)_2]_n$ (MEEP), which showed better cell performance than aluminosilicate-polyether hybrid electrolytes were synthesized; but cell capacity declined rapidly with cycling.

Future Direction

- Project completed.

The objective of this research project is to synthesize polymer electrolytes with improved low-temperature performance, higher cation transport number and useful performance in rechargeable Li/polymer batteries. More recently, tests were performed with cells containing a simple polymer-salt electrolyte, such as $[PN(OCH_2CH_2OCH_2CH_2OCH_3)_2]_n$ (MEEP)-$LiSO_3CF_3$. The test cells contain Li-metal anodes and composite cathodes (70% $Li_xMn_2O_4$, 15%

carbon, and 15% of the respective electrolyte). The cells were charged/discharged at different rates.

$(MEEP)_4LiCF_3SO_3$ was prepared by the ring opening polymerization of purified trimer $(PNCl_2)_3$ at 250°C, followed by nucleophilic substitution with $CH_3OCH_2CH_2OCH_2CH_2ONa$ in tetrahydrofuran (THF). The polymer had been purified by dialysis to remove NaCl impurities and characterized by ^{31}P nuclear magnetic resonance (NMR), Fourier transform infrared (FTIR) spectroscopy, XRD, energy dispersive spectroscopy (EDS), viscosimetry and thermogravimetric analysis (TGA). ^{31}P NMR and FTIR spectroscopy confirmed the identity of the polymer. EDS showed the presence of phosphorus and the absence of chlorine which confirmed the complete removal of NaCl during the purification by dialysis. Dissolution of $LiCF_3SO_3$ into MEEP was carried out with THF as the common solvent. The polymer and the salt in the weight ratio of 4 polymer repeat units to 1 formula unit of salt were thoroughly dried and then dissolved in dry THF under dry nitrogen. A clear solution formed in about one day. Heating was sometimes necessary to assist the dissolution. In order to prepare a solution with a viscosity appropriate for casting films, the concentration was adjusted by evaporation or addition of THF.

The 3 V cathode active material, Li_xMnO_2, was used in cells with $(MEEP)_4LiCF_3SO_3$ because a cyclic voltammogram indicated low stability of this electrolyte at high potentials. Cells containing MEEP-salt complex perform better than cells containing the a-PEO-aluminosilicate complex. Higher current densities can be used during discharge of these cells. However, the increase in discharge rate lowers cell capacity (118 mAh/g at 20 $\mu A/cm^2$ and 73 mAh/g at 30 $\mu A/cm^2$). The reduction of the cell capacity with increased current density is probably the result of incomplete cathode utilization. The use of a thinner cathode layer and better ion transport should improve the performance at high charge/discharge rates.

A drop in cell capacity was observed during repeated charging and discharging. In the first cycle, the capacity of the cell was 122 mAh/g, and after the third cycle the cell capacity was reduced to 105 mAh/g. Also, the MEEP-salt complex did not form a rigid film, and creep of the electrolyte film was detected. As a rule, this deformation lead to a short circuit after few charge/discharge cycles. A spacer material should solve this problem. Chemical crosslinking is another potential solution.

AC impedance tests performed on symmetrical cells with Li electrodes indicate that the total cell resistance increases with time. The Li-electrolyte interface resistance steadily increases with time while the bulk resistance of the MEEP-salt electrolyte is probably due to creep of electrolyte film leading to thinner electrolyte films. It is apparent that the MEEP-salt complex has good potential for application in Li-polymer-electrolyte batteries. However, this potential may be realized only after the low dimensional stability of MEEP and reactivity of MEEP or impurities in MEEP with Li are resolved. Appropriate spacer materials or cross-linked MEEP should overcome the problem of dimensional stability.

New Cathode Materials

M. Stanley Whittingham
Chemistry and Materials Research Center, State University of New York at Binghamton, Binghamton, NY 13902–6000
(607) 777-4623, fax: (607) 777-4623

Objectives

- Synthesize and evaluate oxides of transition metals for alkali-metal intercalation electrodes.
- Identify new intercalation compounds for positive electrodes in advanced nonaqueous secondary batteries.

Approach

- Synthesize metal oxides that have an appropriate crystallographic structure to permit facile intercalation of Li ions.
- Characterize the metal oxide structures by XRD analysis and evaluate materials in electrochemical cells.

Accomplishments

- Cycling studies on $Li_xM_yMnO_2$ (M = Li, Na, K) showed that the highest capacity and longest life was obtained when M = K, which provided the largest interlayer spacing.
- Encouraging results for Li insertion was obtained with layered vanadium oxides $[N(CH_3)_4]_zFe_yV_2O_5 \bullet nH_2O$ (z =1/6, y ≈ 0.1 and n = 1/6) and $Zn_{0.4}V_2O_{5+d} \bullet nH_2O$.

Future Directions

- Continue synthesis and electrochemical studies of vanadium and manganese oxides.
- Use more-stable electrolytes and perform multiple electrochemical cycles on the most-promising oxides.

The objective of this project is to synthesize and evaluate oxides of W, Mo, and first-row transition metals for alkali-metal intercalation electrodes in advanced nonaqueous rechargeable batteries. Mild hydrothermal techniques are being used for the synthesis of molybdenum oxides or, in cases where the hydrotherm-al technique does not lead to compounds in the highest oxidation states, electrochemical oxidation will be used to drive the transition metal to its highest oxidation state.

A layered manganese compound analogous to the layered titanium disulfides was synthesized by the mild hydrothermal aqueous decomposition reaction of potassium permanganate at 170°C. This process has now been extended to the sodium and lithium permanganates, and the decomposition reaction may be represented by:

$$NaMnO_4 + (1\text{-}x+2y)/2H_2O \rightarrow$$

$$Na_xMnO_2 \bullet yH_2O + (1\text{-}x)NaOH + (3+x)/4O_2$$

The lithium permanganate had to be first synthesized; this was accomplished by converting $KMnO_4$ to $HMnO_4$ using an acid ion-exchange column, the permanganic acid was then neutralized giving $NaMnO_4$ by passage down a Na column (the permanganic acid was not isolated, as it has a tendency to explode). The structure of these manganese oxides is indicated in Fig. 22. It is layered and exactly like the disulfides; the alkali ions can be hydrated by either one or two layers of water molecules. The water may be driven out by heating to 150°C; thus all water will be removed on cathode preparation. The hydrothermal decomposition of permanganic acid leads to MnO_2 rather than to a layered $H_3O \bullet MnO_2$. The hydrothermal decomposition of tetramethyl ammonium (TMA)$\bullet MnO_4$ in the presence of Ni salts led to the formation of a totally new structure with the formula $NiMnO_3$ rather than a simple layered manganate as shown in Fig. 22 (see later for a rationale for desiring a layered Ni_yMnO_2).

Structural Analysis. We have completed Rietveld analysis, both X-ray and neutron, on the vanadium oxide phases. In the previous annual report we described the layered tetragonal structure [a=3.705 Å and c=15.80 Å] of the phase $Li_xV_{2-d}O_{4-d} \bullet H_2O$, where δ≤0.2 and x≈0.6, and which contains water between the vanadium oxide sheets. For electrochemical evaluation the water must be removed, which is readily accomplished by heating gently to about 150°C where the lattice contracts from 7.9 to 6.4 Å. The structure of this dehydrated phase is shown in Fig. 23, where the layers between the vanadium oxide square pyramids are very apparent, and the Li resides in the interlayer regions. In the preparation of cathodes for electrochemical evaluation, a mixture of the vanadium oxide, carbon and Teflon

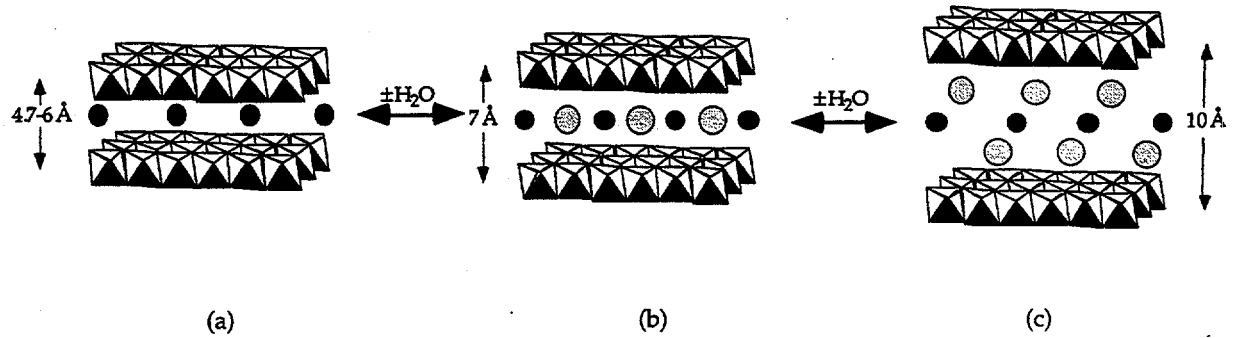

Figure 22. Schematic of layered manganates showing (a) anhydrous material, (b) one water layer, and (c) two water layers. ◌ = H_2O; ● = Li, Na or K ion.

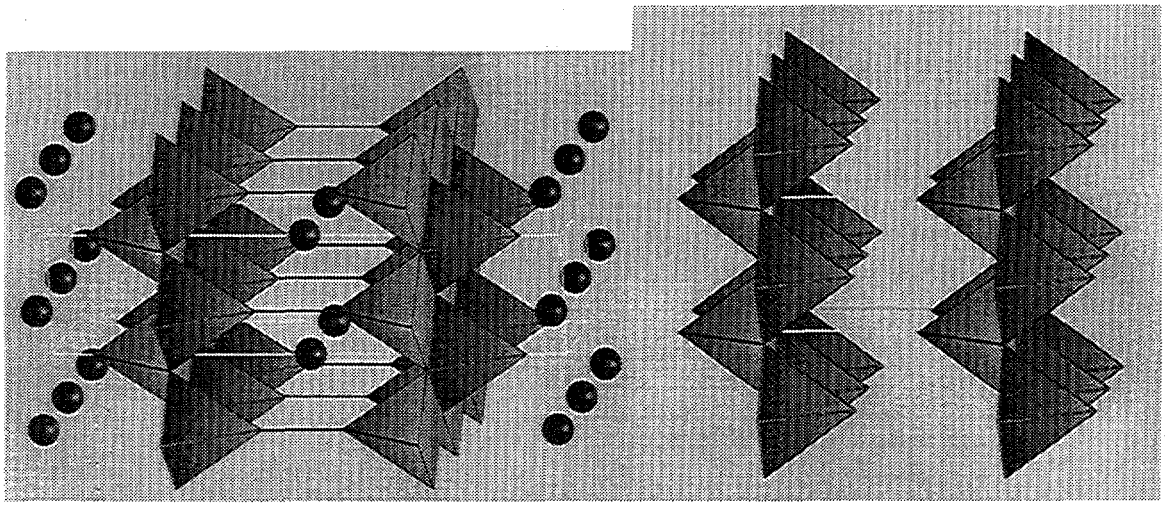

Figure 23. Crystal structure of tetragonal vanadium oxide phase, (left) hydrated phase with water represented by the dark blue spheres, and (right) dehydrated phase.

powder are heated to between 150 and 200°C; X-ray analysis of the formed cathode indicated that the lattice had contracted, confirming that lattice water is not present in the cathodes.

The structures of the TMA compounds, $TMAV_3O_7$ and $TMAV_4O_{10}$, have also been determined, but will not be discussed further as their electrochemical properties were disappointing. The zinc and iron vanadium oxides are believed to have double sheets of vanadium oxide between which lie the Zn, Fe and TMA cations similar to the known δ-V_2O_5 phases; work is continuing on these materials as they look promising electrochemically.

The hexagonal lattice parameters of the rhombohedral manganese oxides, together with their chemical compositions are given in Table 4 .

Reaction with Lithium. Reaction of dehydrated potassium manganese oxide with n-butyl lithium showed an uptake of 1.0 Li/Mn. The electrochemical behavior of all three alkali oxides is shown in Fig. 24. For clarity only the first three cycles of the Li cell are shown. They show a continuous curve indicative of single-phase behavior, $Li_xM_yMnO_2$, similar to that observed in the layered disulfides. These curves of the electrochemical intercalation of Li also suggest that the oxidation state of the manganese is about 3.5, as the initial cell OCV is 3.6 V, close to the value reported for Li insertion into $LiMn_2O_4$. The extended cycling behavior of these hydrothermally formed manganates is still underway.

In the case of the Li compound, $Li_{0.47}MnO_2$, which has an initial electromotive force (emf) of 3.55 V, an additional 0.59 Li is incorporated into the structure during discharges consistent with a maximum of one Li per Mn if all the Li resides on octahedral sites as in $LiTiS_2$. On recharge the Li content is reduced to almost x = 0.2 showing that more than half of the Li originally in the structure can be removed below 4.2 V. The capacity decays

Table 4. Composition and structural data for $(Li,Na,K)_yMnO_2 \cdot nH_2O$

	Lithium	Sodium	Potassium
y	0.47	0.35	0.27
n*	0.74	0.7	0.54
a, Å	2.859	2.852	2.849
c/3, Å *	7.007	7.281	7.179
Dehydrated:			
a, Å	2.85	2.847	2.842
c/3, Å	4.86	5.613	6.440

*The precise c value is dependent on the water content, which varies with the relative humidity.

rapidly after the second cycle as shown in Fig. 25. In addition, if the cell is charged first, the resulting discharge capacity is much worse, as also noted for the Ranciete form of manganese dioxide. For the Na compound 0.47 Li are incorporated in the first discharge, and on recharge more than 0.1 Na ions appear to be removed from the lattice resulting in a larger discharge capacity on the second cycle. The capacity then slowly decays on further cycling. The potassium compound has the highest initial capacity, little extraction of the potassium from the lattice on recharge, and the best maintenance of capacity on cycling. The theoretical capacity based on an average 3 V discharge is 460 Wh/kg, and could probably be improved upon cell optimization. This is essentially the same as $LiCoO_2$ and $LiTiS_2$, as well as to the manganic acid derivatives .

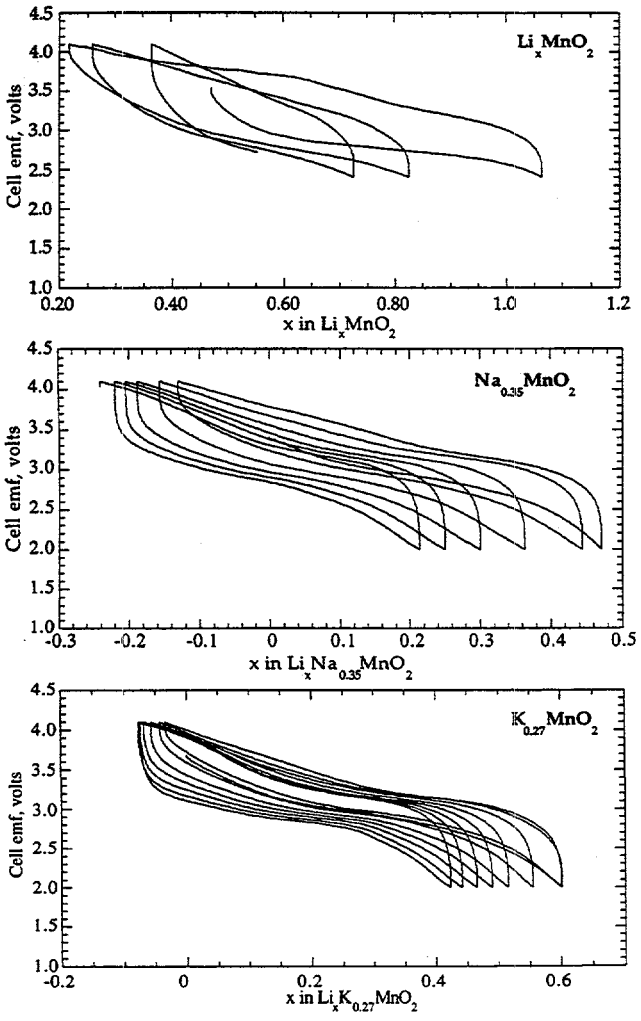

Figure 24. The electrochemical reduction of the lithium, sodium and potassium manganese oxides in a Li cell; the Li metal anode was also used as the reference electrode.

The rapid degradation of capacity during cycling of the Li_xMnO_2 is almost certainly due to diffusion of Mn from the MnO_2 layers to the interlayer region normally occupied by Li. The oxygen lattice in layered Li_xMnO_2 and cubic spinel $LiMn_2O_4$ is identical as shown in Fig. 26. The oxygen ions are arranged in a cubic close-packed manner. The only difference is in the occupancy of the Mn and Li sites, and for x = 0.5, the difference is only in the Mn occupancy. Thus, the Mn ions need only to jump from one octahedral site to the neighboring one; no oxygen ions need to move. The much-better results observed with potassium can be associated with the larger interlayer spacing, 6.39 *vs.* 4.87Å, which is unfavorable for occupancy by Mn ions. The results with the potassium compound leads us to conclude that if the layer structure can be stabilized to prevent Mn migration into the interlamellar region by spacer groups, akin to potassium, then the capacity might approach one Li per Mn atom. To maintain high capacity on cycling this bridging group needs to be immobile so that it cannot be removed on cell charging. Such bridging groups might also allow the oxides to be stabilized in a hexagonal close-packing configuration, which would further stabilize against conversion to the spinel structure. Thus, we tried to incorporate Ni, an electrochemically active ion, into the structure in place of the alkali ion; however, as noted above there was a complete structure change and electrochemical intercalation of Li was minimal, above 2.0 V, even though 1 $Li/NiMnO_3$ could be incorporated chemically. We are continuing to investigate the possibility of stabilizing the layered manganese oxide phase as that offers the best opportunity to cycle 1 Li per transition metal with a relatively small voltage change.

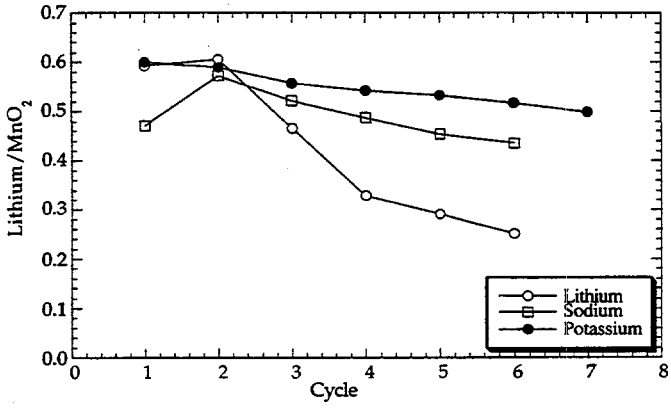

Figure 25. Capacity of the lithium, sodium and potassium manganese oxides during cycling.

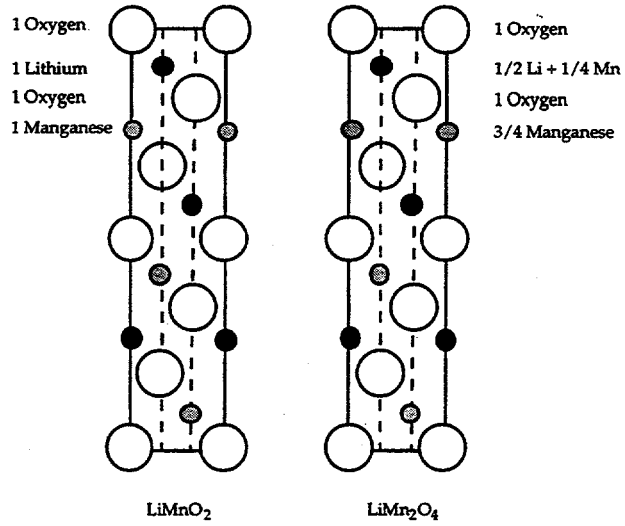

Figure 26. Comparison of the structures of the layered $LiMnO_2$ and the spinel $LiMn_2O_4$, 110 perspectives.

The dried lattice of the $Li_{0.6}V_{2-\delta}O_{4-d} \bullet H_2O$ compound takes up about 1.2 Li/V by reaction with n-butyl lithium. In electrochemical cells this compound has an initial emf of about 3.3 V and readily takes up Li atoms in two well-defined voltage plateaus. On recharge all of this Li is removed on a single continuous curve, as shown in Fig. 27. Moreover, the Li originally in the structure is also removed on recharge, resulting in >0.7 Li being cycled per vanadium after 5 cycles. Removal of all of the Li results in the formation of the new vanadium dioxide phase, VO_2, which has a structure identical to that of V_2O_5 but in the latter 1/3 of all the vanadyl groups are missing in an ordered manner. This phase appears promising as a candidate for the cathode in secondary Li batteries.

We synthesized two new layered vanadium oxides, $[N(CH_3)_4]_zFe_yV_2O_5 \bullet nH_2O$ where z =1/6, y ≈ 0.1 and n = 1/6 and $Zn_{0.4}V_2O_{5+\delta} \bullet nH_2O$. The redox behavior of the Fe compound was determined in an electrochemical cell. The initial open circuit emf was about 3.3 V, Fig. 28. This emf fell steadily as Li was inserted into the structure. On recharge 90% of this Li was recovered. On the second cycle essentially all of this Li could be reinserted and subsequently removed, thus indicating a good overall reversibility of the redox reaction. We are actively pursuing these materials as all of the other vanadium oxides containing organic cations showed minimal reaction with Li in cells. The Zn compound behaved similarly to the Fe one suggesting that the presence of double sheets of V_2O_5 may have a stabilizing influence on the structure.

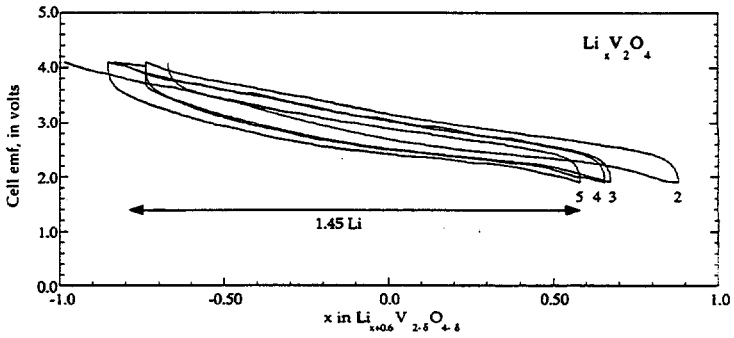

Figure 27. Cycling of $Li_xV_{2-d}O_{4-d}$ cathode in 1 M $LiAsF_6$/PC:DME electrolyte (80% vanadium compound, 10% carbon black, and 10% Teflon binder).

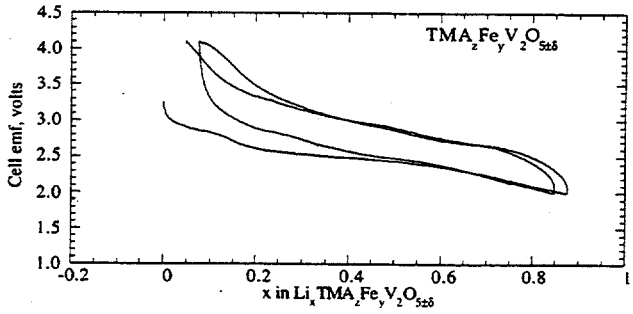

Figure 28. Electrochemical cycling of iron vanadium oxide, using a Li anode, at 0.1 mA/cm^2.

PUBLICATIONS

T. Chirayil, P. Zavalij and M.S. Whittingham, "Hydrothermal Synthesis and Characterization of '$Li_xV_{2-d}O_{4-d}H_2O$'," *Solid State Ionics* **84**, 163 (1996).

R. Chen, P. Zavalij and M.S. Whittingham, "Hydrothermal Synthesis and Characterization of $K_xMnO_2 \bullet yH_2O$," *Chemistry of Materials* **8**, 1275 (1996).

M.S. Whittingham, "Hydrothermal Synthesis of Transition Metal Oxides under Mild Conditions," *Current Opinion in Solid State Science*, **1**, 227 (1996).

P. Zavalij, M.S. Whittingham, E.A. Boylan, V.K. Pecharsky and R.A. Jacobson, "Crystal Structure of Tetramethylammonium Tetravanadium Decaoxide, $N(CH_3)_4V_4O_{10}$," *Z. Krist.* **211**, 464 (1996).

T.A. Chirayil, P.Y. Zavalij and M.S. Whittingham, "A New Vanadium Dioxide Cathode," *J. Electrochem. Soc.* **143**, L193 (1996) .

M.S. Whittingham, R. Chen, T. Chirayil and P.Y. Zavalij, "Cathode Materials For Advanced Batteries," *Proceedings of Exploratory Research and Development of Batteries for Electric and Hybrid Vehicles*, Vol. **96-5**, 76, Electrochemical Society Meeting, San Antonio, TX, October, 1996.

R. Chen, T. Chirayil and M.S. Whittingham, "The Hydrothermal Synthesis of Sodium Manganese Oxide and a Lithium Vanadium Oxide," *Solid State Ionics* **86-88**, 1 (1996).

E.A. Boylan, T. Chirayil, J. Hinz, P.Y. Zavalij and M.S. Whittingham, "Vanadium Oxides Synthesized Using the Tetramethylammonium Ion: An Addendum." *Solid State Ionics* **90**, 1 (1996).

Lithium Polymer Rechargeable Batteries with Lithium Manganese Oxide Cathodes

Rick Howard
Covalent Associates, Inc., 10 State Street, Woburn MA 01801
(617) 938-1140, fax: (617) 938-1364

Objectives

- Identify low-cost, high-performance Mn-based electrode material for Li rechargeable batteries.
- Demonstrate charge/discharge cycling of Mn-based electrodes in $LiPF_6$ and Li methide in solution and in polymer electrolytes.

Approach

- Investigate process control and chemical analyses of electrode materials to confirm single-phase product.
- Evaluate electrode performance using Li/$LiMn_2O_4$ test cells.

Accomplishments

- Fabricated test cells with $LiCr_{0.02}Mn_{1.98}O_4$/$LiPF_6$-EC-DEC/Li foil which achieved an initial discharge capacity of 118 mAh/g, falling to 105 mAh/g after 486 cycles, when the cell failed.
- Established that low levels of Cr(III) adduct stabilized $LiMn_2O_4$ against electrochemical degradation during cell cycling.
- Prepared polymer electrolytes containing Li methide and γ-$LiAlO_2$ that exhibited improved performance.

Future Direction

- Project completed.

The major objective of this research is to develop an improved $LiMn_2O_4$ spinel cathode material for rechargeable Li batteries. Candidate cathode materials were prepared by a solid-state reaction at 700-800°C. Only chromium admetal yielded single-phase spinels that exhibited stable capacities, with the higher Cr levels yielding lower discharge capacities, as expected. The preferred cathode material was $LiCr_{0.02}Mn_{1.98}O_4$, which provided 108-112 mAh/g reversible capacity for at least 100 cycles. Unmodified $LiMn_2O_4$ showed up to 130 mAh/g initial reversible capacity but capacity fade rapidly diminished performance levels to 80% of first-cycle values in only 100 cycles.

The inclusion of a Cr(III) modifier in $LiMn_2O_4$ caused a decrease in initial discharge capacities but resulted in a surprisingly stable output. With 7 mol% Cr (relative to Mn), reversible capacity started at 86 mAh/g and showed a slight improvement to 91 mAh/g after 118 cycles. This trend continued similarly down to 1 mol% Cr,

which produced 109 mAh/g initially and 111 mAh/g after 80 cycles. The adduct is Cr^{+3}, a non-toxic, water-insoluble oxidation state of Cr. In contrast, Cr^{+6} is toxic and carcinogenic.

The pronounced improvements in capacity retention with 1% Cr admetal were also observed at elevated (55°C) temperatures. Unmodified $LiMn_2O_4$ lost half of its capacity in only 50 cycles, whereas the 1% Cr material retained >80% over the same period. Electrolyte breakdown was also a primary cause of performance decline, likely accelerated by the Li metal anode. Capacity decline at 55°C was exacerbated by trace H_2O.

Test cells were prepared as $LiCr_{0.02}Mn_{1.98}O_4$/ $LiPF_6$-EC-DEC/Li foil, with strict attention to the issue of H_2O contamination. The result was a system with excellent capacity stability. Initial discharge capacity was 118 mAh/g, falling to 105 mAh/g after 486 cycles, when the cell failed. This calculated to an average fade rate of 0.024%/cycle. Faradaic efficiencies were also unusually high, averaging 99.6%.

The physical aspects of unmodified and Cr-doped $LiMn_2O_4$ differed only slightly. SEM photos of $LiMn_2O_4$ showed spherical, 10-75 μm particles at low magnification and a porous structure comprising 1 μm crystallites at 5000X. Only with 7% Cr was there any noticeable glazing or sintering of the microcrystals. Surface areas clustered around 2.5 m^2/g, regardless of the Cr content. The tap densities (1.5-1.6 g/cm^3) were also unaffected by the presence of the admetal.

The composite polymer electrolyte (CPE) contained PEO and liquid polyethylene glycol-dimethoxyethane (PEG-DME) polymers with either $LiPF_6$ or Li methide salts and various loadings of γ-$LiAlO_2$. $LiPF_6$ was immediately ruled out as a viable ingredient when it reacted with the polymers during the 60°C annealing step, creating an intractable solid mass. Starting at 10% ceramic filler, CPEs containing Li methide showed increasing conductivity and enhanced performance, up to 50% γ-$LiAlO_2$. Ambient-temperature results were marginal, and only slow charge/discharge rates were tolerated.

CPE performance was markedly improved either by raising the cell temperature (to 55°C) or adding a few drops of liquid electrolyte to the CPE disk during cell construction (preferred). At least 30% γ-$LiAlO_2$ was required, and 8-10% Li methide levels were optimum. High-temperature cycling with "dry" CPEs resulted in rapid capacity fade that was likely caused by electrochemical polymer degradation leading to a buildup of an anodic interface barrier that restricted Li^+ transport. A Li/$LiMn_2O_4$ cell with a few drops of liquid added to 40% γ-$LiAlO_2$ yielded results equivalent to liquid electrolyte systems: >130 mAh/g reversible capacity at 0.1 mA/cm^2. Porosity problems, leading to premature cell demise by dendrites, was ameliorated but not completely overcome.

PUBLICATIONS

S.H. Lu, W.F. Averill, A.D. Robertson and W.F. Howard, Jr., "Comparisons of $LiMn_2O_4$-Based Intercalation Cathodes with $LiPF_6$ and Li Methide Electrolyte Solutions," in *Proceedings of the 13th Intl. Seminar, Primary and Secondary Battery Technol. and Appl.*, Boca Raton, FL (March 4-7, 1996).

W.F. Howard, Jr., S.H. Lu, W.F. Averill and A.D. Robertson, "Comparison of $LiPF_6$ and Li Methide Electrolytes Using $LiMn_2O_4$ Cathode Materials," in *Proceedings of the 37th Power Sources Conf.*, Cherry Hill, NJ (June 17-20, 1996), pp. 235-238.

A.D. Robertson, S.H. Lu, and W.J. Howard, Jr., "Fundamental Studies of Cr^{3+} Stabilized $LiMn_2O_4$ Cathode Materials," in *Proceedings of the 10th IBA Battery Matl. Symp.*, Tucson, AZ (October 1-4 , 1996).

D. CROSS-CUTTING RESEARCH

Cross-cutting research is carried out to address fundamental problems in electrochemistry, current-density distribution and phenomenological processes, solution of which will lead to improved electrode structures and performance in batteries and fuel cells.

Analysis and Simulation of Electrochemical Systems

John Newman (Lawrence Berkeley National Laboratory)
201 Gilman Hall, MC 1462, University of California, Berkeley CA 94720
(510) 642-4063, fax: (510) 642-4778

Objectives

- Improve the performance of electrochemical cells used in the interconversion of electrical energy and chemical energy by identifying the phenomena that control the performance of a system.
- Identify important parameters which are crucial to the optimization of an advanced secondary battery.

Approach

- Utilize electrochemical engineering principles and advanced computation techniques to develop mathematical models.

Accomplishments

- Slow charge/discharge potential transients, cyclic voltammetry, and potential step data have been collected using a nickel hydroxide-hydrogen thin-film cell. These data compare well with output from the numerical model.
- The influence of side reactions on relaxation phenomena in cells containing $Li_xMn_2O_4$ was investigated experimentally and with mathematical modeling.

Future Directions

- Investigate secondary effects in the Li/polymer cell, such as film formation and volume changes .
- Investigate the behavior of batteries and supercapacitors subject to the performance demands expected for EVs, including failure modes.
- Continue experimental studies to provide the relevant physical properties to verify the mathematical models.

This program involves fundamental investigations of the transport and interfacial phenomena important in electrochemical systems. Results of this work are used to analyze experimental data, to identify important system parameters, and to aid in the design and scale-up of electrochemical systems. The approach taken is to develop a detailed mathematical model of the electrochemical device using the principles of transport phenomena, reaction kinetics, and thermodynamics. The mathematical models are developed to be as general as possible without unnecessary mathematical or physical approximations. The resulting sets of coupled equations are then solved numerically, which permits the complex interactions between phenomena to be treated. Experimental work may then be used to confirm and refine the mathematical models and to determine the physical parameters necessary for a complete, quantitative understanding of the system.

Experimental techniques and computer simulations have been developed and applied to several systems to elucidate the phenomena which govern the behavior of electrode and electrolyte materials. Once these phenomena have been identified and the corresponding physical properties measured, a cell or device which uses

these materials can be optimized. The systems under study at present are based on materials under consideration for advanced battery systems: solid electrolytes for use in Li batteries and $LiMn_2O_4$ and NiOOH electrode materials. In addition to these studies of physical properties, computer simulations are being refined to model the performance of electrochemical devices under the load requirements of hybrid EVs.

Transport properties in electrolyte materials are necessary to determine the ohmic drop and concentration polarization in batteries. The galvanostatic-polarization method was developed in this group to determine the transference number in solid electrolytes, as other traditional methods can not be applied to these systems. The technique involves no assumptions about the ideality of the solution. The galvanostatic-polarization method has since been applied to measure the transference number of Li in lithium trifluoromethanesulfonate with poly(ethylene oxide) as the solvent at 100°C. The salt diffusion coefficient was measured by the method of restricted diffusion and the conductivity was measured by standard ac-impedance techniques. Thus, by determining the transference number, diffusion coefficient, and conductivity, a complete set of transport properties for the electrolyte was determined. This work is being continued to examine more concentrations and other electrolytes.

Electrode materials are also being studied. Mathematical models have been developed to model the intercalation process in both NiO and $LiMn_2O_4$ electrodes, and to clear up the ambiguity of the state of charge when there are side reactions occurring in parallel with the intercalation reaction. Work has been done to determine the open-circuit potential of $Li_xMn_2O_4$ intercalation electrodes as a function of state of charge and to measure the ion diffusion coefficient in nickel hydroxide electrodes. Both of these systems are plagued by side reactions, which reduce current efficiency and obscure the physical properties which are to be measured. Most standard experimental techniques are based upon the assumption that the current efficiency for the desired reaction is 100%. In the study of these electrodes, experimental techniques have been combined with numerical simulations to ascertain the influence of side reactions and, subsequently, to back out the physical properties. Work is continuing on these electrodes to explore the effects of particle-size distributions on the performance of the electrode.

In the $Li_xMn_2O_4$ system, the influence of side reactions on relaxation phenomena in these cells is investigated experimentally and with a mathematical model. The influence of these reactions on cycling will also be investigated. The contributions of charge-transfer resistance, mass-transfer limitations, and side reactions of the nickel hydroxide-hydrogen cell are all included in the numerical model. The model's framework and objectives are applicable to most rechargeable cells employing an intercalation material. Slow charge/discharge potential transients, cyclic voltammetry, and potential-step data have been collected using a nickel hydroxide-hydrogen thin-film cell. These data compare well with output from the numerical model described above. Future experimental work includes surface and thickness characterization of the nickel hydroxide thin films using SEM, profilometry, and "wet" analytical chemistry.

The methods that have been used by previous workers in the measurement of ion diffusion in solid nickel hydroxide are being critically analyzed. Unlike previous studies, the present work does not assume *a priori* that mass transfer within the solid nickel hydroxide controls the nickel hydroxide-hydrogen cell behavior, and therefore provides a truer assessment of the complex behavior of this rechargeable cell.

The influence of the exchange current density on the reaction-rate distribution in porous intercalation electrodes at short times has been investigated with a linearized model. Asymptotic solutions have been developed for short, intermediate, and moderately long times. These asymptotic solutions have helped to elucidate the importance of the concentration overpotentials in the electrolyte and solid phases on the redistribution of the reaction rate. The concentration overpotentials quickly spread the reaction out.

Improvements on the basic Li battery model will involve the inclusion of the possibility of salt precipitation inside of the separator. There is growing evidence that this is an important phenomenon in concentrated polymer electrolyte systems.

Computer programs which already describe the behavior of Li batteries are being modified and extended to simulate the performance of batteries under cycling and load profiles for hybrid EVs. Work is also being renewed on supercapacitors, both those based upon double-layer charging and those using Pt-Ru electrodes, which exhibit the characteristic known as pseudocapacitance. These devices will also be modeled to determine their performance under the load expected for a hybrid EV driving profile.

PUBLICATIONS

J. Newman, "Electrostatic Systems and Electrochemical Systems," *Proceedings of the Symposia on Fundamentals of Electrochemical Process Design: A Tutorial*, J.B. Talbot, J.M. Fenton, B.E. Conway and B.V. Tilak, eds; and *Anodic Processes: Fundamental and Applied Aspects*, **PV 95-11**, pp. 141-154, Pennington, New Jersey, The Electrochemical Society, 1995. LBL-37457.

B. Paxton and J. Newman, "Variable Diffusivity in Intercalation Materials: A Theoretical Approach," *J. Electrochem. Soc.*, **143**, 1287 (1996).

B. Pillay and J. Newman, "The Influence of Side Reactions on the Performance of Electrochemical Double-Layer Capacitors," *J. Electrochem. Soc.*, **143**, 1806 (1996).

M. Doyle, J. Newman, A.S. Gozdz, C.N. Schmutz and J-M. Tarascon, "Comparison of Modeling Predictions with Experimental Data from Plastic Lithium Ion Cells," *J. Electrochem. Soc.*, **143**, 1890 (1996).

S. Umino and J. Newman, "Temperature Dependence of the Diffusion Coefficient of Sulfuric Acid in Water," August 1996. LBNL-39212.

L. Rao and J. Newman, "Heat-Generation Rate and General Energy Balance for Insertion Battery Systems," October 1996. LBNL-39456.

R. Darling and J. Newman, "On the Short-Time Behavior of Porous Intercalation Electrodes," November 1996. LBNL-39581.

Corrosion of Current Collectors in Rechargeable Lithium Batteries

James W. Evans (Lawrence Berkeley National Laboratory)
585 Evans Hall, MC 1760, University of California, Berkeley CA 94720
(510) 642-3807, fax: (510) 642-9164

Objectives

- Examine corrosion of current collectors in Li-polymer and Li-ion batteries.
- Develop corrosion-resistant collectors and/or corrosion inhibition approaches.

Approach

- Use DC and AC electrochemical techniques to develop understanding of the corrosion behaviour of current collectors and corrosivity of various electrolytes.
- Identify corrosion of current collectors in Li batteries under different charge conditions by SEM/energy dispersive X-ray (EDX) analyses.
- Explore corrosion-resistant alloys by ion-implantation or sputter deposition.

Accomplishments

- The results indicate that Al is the most corrosion-resistant of the common collector materials in polymer electrolytes, however, localized/pitting may affect the long-term reliability of Li-polymer batteries
- It was found that, after short-term normal cycle tests of Li/V_6O_{13} cells, a small amount of corrosion pits appeared on Al collectors, and serious pitting corrosion occurred after overcharging.
- Tungsten-implanted Al was shown to be highly resistant to pitting corrosion during repeated potentiodynamic scans and during cycle tests in Li/V_6O_{13} cells.

Future Directions

- Continue corrosion tests in Li-polymer batteries and examine current collector corrosion in Li-ion batteries with various nonaqueous electrolytes.
- Continue exploration of corrosion-resistant alloys and investigate the effect of surface treatments on corrosion.
- Develop understanding of corrosion mechanism/products by Auger electron spectroscopy (AES), electron spectroscopy for chemical analysis (ESCA), and/or surface-enhanced Raman spectroscopy (SERS).

Common current collector materials (without surface treatment or even with some sorts of treatment) may be seriously corroded during charge/overcharge of Li batteries. The solution to corrosion problems will increase the long-term reliability of, and maximize the service life of, Li batteries. The objectives of this project are to examine the corrosion of current collectors, to evaluate the corrosivity of different Li salts and electrolyte solutions, and to explore corrosion-resistant collector materials and materials-processing technologies.

To develop an understanding of the corrosion of Al (the most corrosion-resistant materials as compared with Cu, Ni, and common stainless steels) in a typical polymer electrolyte (PEO)-lithium imide salt), electrochemical corrosion techniques (potentiodynamic scan, potentiostatic hold, cyclic polarization, and AC impedance spectroscopy) were applied and the corrosion rates of Al in a corrosion cell (consisting of an Al working electrode, and Li counter and reference electrode), under different potentials and during repetitive potential scans were determined. The results indicate that Al is a corrosion-resistant material when corrosion proceeds uniformly. However, localized/pitting corrosion on Al was identified by SEM.

To study the corrosion of Al collector during battery operation, examination of Al collectors in Li/PEO)-lithium imide salt/V_6O_{13} (composite electrode) cells, after charges at various potentials, was conducted with SEM. This investigation indicated that after short-term normal cycle tests, a small amount of corrosion pits appeared. However, after overcharging, serious pitting corrosion occurred. Therefore, the pitting corrosion on Al current collectors will affect the long-term reliability of this battery system.

A search for corrosion-resistant Al alloys was carried out. Tungsten-implanted Al, during potentiodynamic polarization, showed corrosion currents of a magnitude similar to that on Al (much less than those on Cu, Fe, Ni, and 304 stainless steel). After repeated potentiodynamic scans, the corrosion currents decreased, compared to Al, possibly due to the formation of more protective corrosion product films. The SEM microphotographs of the W-Al alloys after potentiodynamic/potentiostatic scans in corrosion cells and after cycle tests in battery cells did not show visible corrosion pits. Therefore, the W-implanted Al can be used as a corrosion-resistant collector in the battery.

Further work will include examination of current collector corrosion in Li-ion batteries with various nonaqueous electrolytes, investigation of surface treatments as an approach to corrosion inhibition, exploration of corrosion-resistant alloys, and development of understanding of corrosion mechanism/products by *ex* or *in situ* surface-analysis techniques such as AES, ESCA and SERS.

PUBLICATION

Y. Chen, T.M. Devine and J.W. Evans, "Corrosion of Aluminum Current Collector in the Li/PEO-$LiN(CF_3SO_2)_2/V_6O_{13}$ Battery," in *Proceedings of the Symposium of Lithium Polymer Batteries*, J. Broadhead and B. Scrosati, eds., **PV96-17**, The Electrochemical Society Inc. Pennington, NJ (1996).

Electrode Surface Layers

Frank R. McLarnon
90-1142 , Lawrence Berkeley National Laboratory, Berkeley CA 94720
(510) 486-4636, fax: (510) 486-4260

Objectives

- Apply advanced *in situ* and *ex situ* characterization techniques to study the structure, composition and mode of formation of surface layers on electrodes used in rechargeable batteries.
- Identify film properties that improve the rechargeability, cycle-life performance, specific power, specific energy, stability and energy efficiency of electrochemical cells.

Approach

- Apply sensitive techniques such as ellipsometry, Raman spectroscopy, and impedance analysis SEM to monitor the formation of surface layers on secondary battery electrodes.
- Incorporate foreign ions in porous nickel oxide electrodes to improve cycle performance in an alkaline electrolyte.

Accomplishments

- Quantitative analysis of the SER spectra of a $Ni/Ni(OH)_2$ electrode showed that the initial α-$Ni(OH)_2$ phase is only partially converted into β-$Ni(OH)_2$ during cycling.
- Cyclic voltammetry of a TiO_2-modified Ni electrode shows that TiO_2 addition does not significantly shift the O_2-evolution potential, contrary to expectations.

Future Directions

- Complete series of Raman and electrochemical experiments to characterize TiO_2-modified Ni electrode.
- Continue search for Ni substrate surface modification method that could improve the performance and efficiency of thin-film Ni electrodes.
- Continue effort to characterize film formation on carbonaceous materials in nonaqueous electrolytes using ellipsometry and infrared spectroscopy.

Advanced *in situ* and *ex situ* characterization techniques are being used to study the structure, composition and mode of formation of surface layers on electrodes used in rechargeable batteries. The primary objective of this research is to identify film properties that improve the rechargeability, cycle-life performance, specific power, specific energy, stability and energy efficiency of electrochemical cells. The present research seeks to characterize the transformation of surface phases that accompanies the charging and discharging of Ni electrodes in alkaline electrolytes and Li electrodes in nonaqueous electrolytes.

Nickel Electrodes. We used *in situ* surface Raman spectroscopy in conjunction with electrochemical techniques to characterize in detail thin films of $Ni(OH)_2$ cathodically deposited on a Ni substrate. Raman spectra of reduced as well as oxidized active material were obtained for film thicknesses varying from 100 to 1000 equivalent monolayers of $Ni(OH)_2$ as determined from the Faradaic charge for the galvanostatic deposition and the charge for the cyclic voltammetric oxidation of $Ni(OH)_2$. For the thicker films, Raman bands at 450 cm^{-1} and at 480 and 560 cm^{-1} were obtained for the reduced and oxidized films, respectively, which are in perfect agreement with the literature data and the previously reported results for the thinner films.

Numerical deconvolution of the spectra of oxidized active material and analysis of the dependence of the 480/560 cm^{-1} band intensities as a function of number of charge/discharge cycles showed that we could characterize cycle-dependent changes in the oxidized film by unique Raman signatures. Taking into account the widely postulated reaction scheme proposed by Bode, the relative 480/560 cm^{-1} peak intensity ratio decline could be attributed to the conversion of γ-NiOOH to β-NiOOH with aging. This was the first example of using Raman spectroscopy measurements and analysis to provide quantitative information about

the structural changes in oxidized Ni films that accompany charge-discharge cycling.

Analysis of SER spectra of reduced active material as a function of the film thickness and the number of charge/discharge cycles was also carried out. The spectral changes following the electrode cycling supported the idea of the transformation of α to β-$Ni(OH)_2$ however, prolonged cycling resulted in the formation of some new $Ni(OH)_2$ phases which were represented by new bands on Raman spectra. Interestingly, formation of new phases upon electrode cycling was more pronounced for thicker films. The quantitative analysis of the SER spectra showed that precursor α-$Ni(OH)_2$ phase is only partially converted into β-$Ni(OH)_2$ during cycling. On the other hand, the position of "new Raman bands" which arise on the spectra with increasing number of charge/discharge cycles corresponds to the bands observed on the *ex situ* spectra of chemically synthesized α-$Ni(OH)_2$ materials. We determined that aging and/or cycling of the Ni electrode leads to an α/β phase interconversion process which is in agreement with the widely postulated Bode model but also we were able to detect the structural changes which occur within the single α phase. We assume that this effect is due to the dehydration, and consequently, recrystallization of the active material in the film.

Another aim of our work was to continue our research on film modification by anatase TiO_2 addition to cathodically precipitated $Ni(OH)_2$ film. One of the postulated reasons of the decay of the Ni electrode capacity and its mechanical destruction is the O_2-evolution reaction, which proceeds in parallel to anodic oxidation of $Ni(OH)_2$. TiO_2 appears to be particularly well suited for such an attempt because of its high overpotential toward O_2 evolution, good stability in alkaline media as well as the facility of preparing the thin polycrystalline film. The electrochemical behavior of electrochemically precipitated thin-film $Ni(OH)_2$ electrodes in alkaline NaOH solution was investigated by means of cyclic voltammetry (CV) and Raman spectroscopy and the effect of a thin overlayer of TiO_2 on the kinetics of charge-discharge cycling and consequently, the structure and phase composition of the charged and discharged films, was studied. The modified Ni electrodes were prepared according to the method described for thin-layer TiO_2 photoanodes. The freshly precipitated, thick (200 mC/cm^2) $Ni(OH)_2$ film was dried in air at room temperature and a drop of a suspension of anatase TiO_2 in dimethyl-formamide (DMF) containing dissolved polyvinylidene fluoride (PVDF) was deposited onto the spinning Ni electrode and dried in air for 2 h at 50°C. The amount of the TiO_2 and PVDF, and consequently the thickness of the overlayer, could be adjusted by changing the spinning speed of the Ni electrode. Raman spectra of solid samples of chemically synthesized TiO_2 were examined in air not only to distinguish between its two structural forms, *i.e.*, anatase and rutile, but also to gain information about specific vibrations assigned to crystalline forms of TiO_2 which may contribute to the *in situ* signal for the modified Ni electrode. Both the surface chemistry of TiO_2 and the kinetics of reactions occurring at TiO_2 are markedly affected by its crystalline structure. The Raman spectrum of the reagent-grade TiO_2 powder which was used in this study shows that it consist mainly of anatase form which prevails over rutile.

We then determined the effect of the TiO_2 overlayer on the electrochemical response of the Ni electrode. The presence of the polymer-bonded layer of TiO_2 on the top of the $Ni(OH)_2$ layer significantly reduces the rate of transformation of precursor active material into disordered β-phase materials. However, it did not prevent the capacity loss of the Ni electrode with the increasing number of charge/discharge cycles, suggesting another electrode failure mechanism other than the α-to-β phase transition. Surprisingly, examination of the cyclic voltammograms of the modified Ni electrode shows that TiO_2 addition does not significantly shift the O_2-evolution potential. On the other hand, increasing the thickness of the overlayer has a substantial effect on the kinetics of the charging/discharging process. The rate of redox reaction is slower due to a polymer ion diffusion barrier at the electrode interface. Interestingly, the polymer overlayer apparently has very good hydrophobic properties while it is still permeable to ion transport. It could be considered as a separator material for use in multilayer battery technology.

The electrochemical precipitation of $Ni(OH)_2$ is recognized as an efficient process for the incorporation of active material into the positive electrode of rechargeable alkaline batteries. It has been shown that cathodically impregnated sintered Ni electrodes have superior electrochemical properties compared to those made by conventional pasting or chemical precipitation processes. However, the mechanism and kinetics of this process are still poorly understood, in particular with regard to how the various operating conditions [*e.g.*, temperature, current density and $Ni(NO_3)_2$ concentration] affect the

efficiency of the precipitation process, the structure of the precipitated film, and the performance and durability of the fabricated electrode. The electrodeposition of $Ni(OH)_2$ films involves the electrochemical reduction of NO_3^- ions at a Ni substrate and the consequent local generation of OH^- ions. The OH^- production increases the local pH and thereby initiates a two-step precipitation of $Ni(OH)_2$ on the electrode surface, involving an intermediate $Ni_4(OH)_4^{4+}$ species. Nickel hydroxide does not precipitate as pure $Ni(OH)_2$; there exists experimental evidence that both solvent and ions are incorporated in the film as it is deposited. The quantity of intercalated ions and water trapped in the film, and thus the structure of the precursor nickel hydroxide material, depend on the film growth rate, which is determined by the deposition conditions.

The objective of our work was also to determine the effect of cathodic current density on the efficiency of the electrochemical deposition of $Ni(OH)_2$ by transient *in situ* measurement of the optical constants of the deposited film. The $Ni(OH)_2$ films were deposited at ambient temperature onto a mirror-finished surface of a Pt electrode from a solution of 0.1 M $Ni(NO_3)_2$ at selected current densities of 0.075, 0.15, 0.3 and 0.6 mA/cm^2. The precipitation was continued until a charge of 380 mC/cm^2 was passed in each of the four experiments. An automatic self-compensating ellipsometer was used to monitor *in situ* the $Ni(OH)_2$ deposition process. Plots (Fig. 29) of the measured ellipsometric parameters, Δ and Ψ. of the four $Ni(OH)_2$ films *vs.* charge density revealed marked differences in the nature of the films as well as the kinetics of the deposition process. Numerical analysis of the ellipsometric data allowed us to determine the thicknesses and optical constants of the films. The four cathodic deposition experiments gave analogous sets of data, although plots of the optical parameters, Δ and Ψ, appear quite different due to the particular optical properties of the films. The initial stage of $Ni(OH)_2$ deposition (*i.e.*, up to 100 mC/cm^2) at all current densities produced films with very similar optical constants. Interestingly, the longer the process was carried out, the more pronounced the differences in optical properties of the films became. We postulate that two factors are primarily responsible for this phenomenon: solvent and ion incorporation into the film, and changes in the $Ni(OH)_2$ layered lattice spacing. Electrochemical precipitation at 0.3 mA/cm^2 produced a homogeneous non-optically-absorbing layer of $Ni(OH)_2$ which grew steadily with little change in optical constants of the film. Deposition at both higher and lower current densities generated optically denser films. The low deposition rate at low current density generates dense films with small interlamellar distance; however, at high current densities as the deposition rate increases, the ions and solvent molecules of the electrolyte become trapped within the film.

Lithium-Carbon Electrodes. We have characterized pyrolytic carbon films on Si substrates prepared at different temperatures (700, 900 and 1050°C) and with various thicknesses (from 1-3 μm) with a Woollam M-44 ellipsometer. Preliminary studies indicated that the apparent optical constants of pyrolytic carbon films lie between those for ordinary and extraordinary indices of crystalline graphite, and thereby suggest an amorphous structure model for such films. We detected a difference between apparent extinction coefficients for samples treated at different temperatures – the higher the treatment temperature, the larger the extinction coefficients. The reason for this trend is unexplained at this time. A test cell for *in situ* characterization of the formation and growth of interfacial layer on carbon films has been designed. Preliminary simulation calculations predict the necessity to develop an improved methodology to perform ellipsometric measurements with high accuracy.

PUBLICATIONS

S. Anders, A. Anders, I. Brown, F. Kong and F. McLarnon, "Surface Modification of Nickel Battery Electrodes by Cobalt Plasma Immersion Ion Implantation and Deposition," *Surface & Coatings Technology*, **85**, 75 (1996).

R. Kostecki, and F. McLarnon, "Electrochemical and *In Situ* Raman Spectroscopic Characterization of Nickel Hydroxide Electrodes. I. Pure Nickel Hydroxide," *J. Electrochem. Soc.*, **144**, 485 (1997).

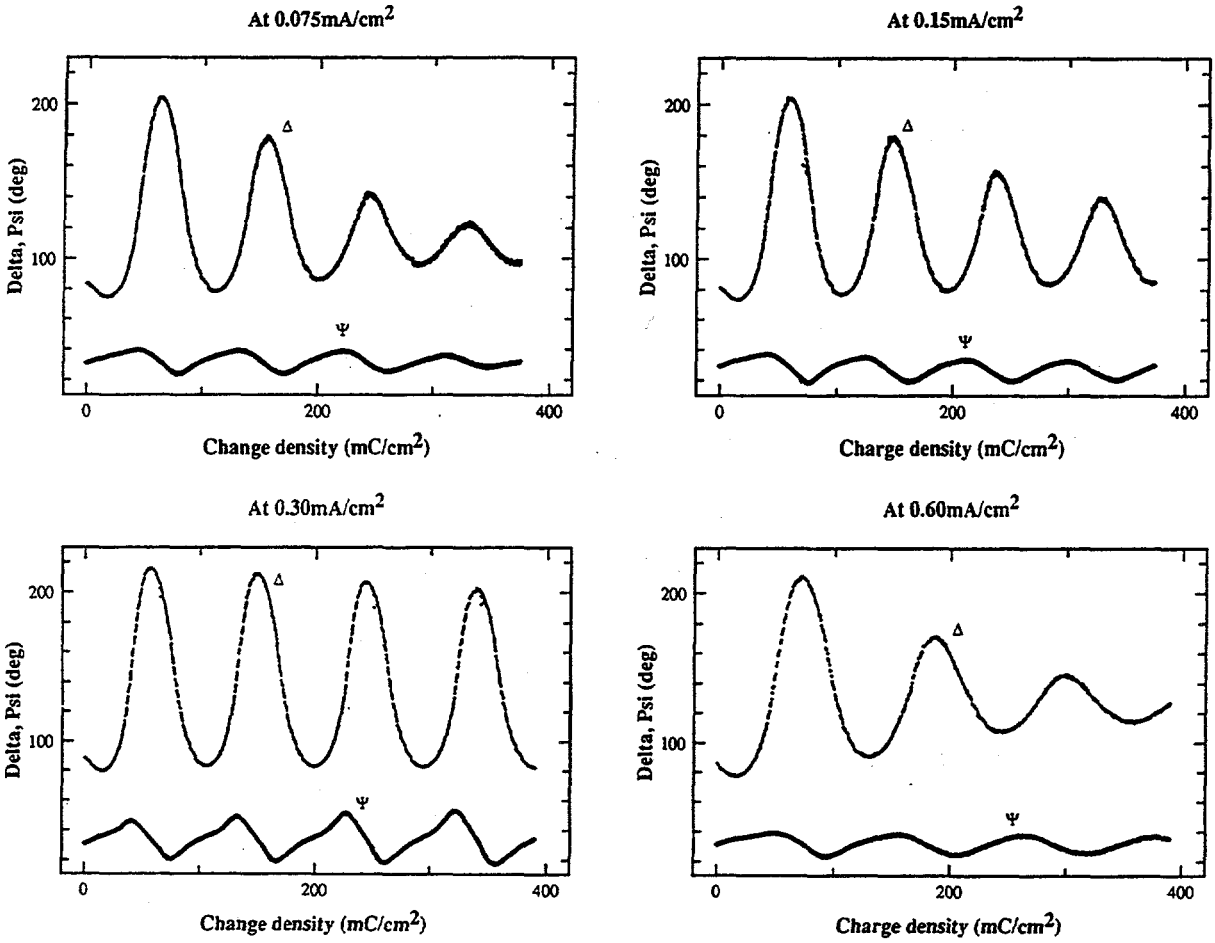

Figure 29. Variation of ellipsometer parameters, Δ and Ψ, with charge passed during the electrochemical precipitation of $Ni(OH)_2$, recorded for four different current densities at a constant illumination wavelength of 500 nm. Uniform periodic behavior is observed only at 0.3 mA/cm^2, indicating uniform $Ni(OH)_2$ film properties at this current density. Decaying periodic behavior is observed at higher or lower current densities, indicating non-uniform film properties.

IV. FUEL CELL RESEARCH

The objectives of this program element are to characterize and improve materials for fuel cells for transportation applications. This research includes projects in several areas of electrochemistry: fuel-cell testing, fuel processing, fuel-cell component characterization and theoretical studies. Fuel cell research was not included in the ETR Program as of FY 1997.

Electrode Kinetics and Electrocatalysis

Philip N. Ross, Jr.
2-100, Lawrence Berkeley National Laboratory, Berkeley CA 94720
(510) 486-6226, fax: (510) 486-5530

Objectives

- Develop an atomic-level understanding of the processes taking place in complex electrochemical reactions at electrode surfaces.
- Determine the relationship between the kinetics of electrode processes and the atomic structure of the electrode surface by using a variety of surface- or bulk-sensitive techniques.

Approach

- Employ low-energy electron diffraction (LEED) to study single crystals; high-energy electron microscopy (HREM) in the case of carbon electrode materials; and EXAFS for organometallic catalysts.
- Utilize low-energy ion scattering (LEIS) and AES to study the composition of sputtered and ultrahigh vacuum (UHV)-annealed polycrystalline Pt-Ru and Pt-Sn bulk alloys for methanol and CO oxidation electrocatalysis.

Accomplishment

- It was found that both the surface and bulk composition of $Pt_{75}Mo_{25}$ alloy was the same.

Future Directions

- Continue the study of CO tolerance in low-temperature acid fuel cells and in parallel begin the examination of methanol oxidation on one or more new Pt alloy systems.
- Begin experimental work investigating CO and H_2/CO electrooxidation based on non-Pt catalysts.

The objective of this project is to develop an atomic-level understanding of the processes taking place in complex electrochemical reactions at electrode surfaces. Physically meaningful mechanistic models are essential for the interpretation of electrode behavior and are useful in directing the research on new classes of materials for electrochemical energy conversion and storage devices.

The electrochemical oxidation of hydrogen in the presence of carbon monoxide (0.05–2%) on a well-characterized $Pt_{75}Mo_{25}$ alloy surface was examined using the rotating disk electrode technique in 0.5 M H_2SO_4 at 333 K. The surface composition of this alloy determined by LEIS after sputter cleaning and annealing in UHV was essentially the same as the bulk. The shapes of the polarization curves are qualitatively similar to those for the $Pt_{50}Ru_{50}$ alloy examined previously: a high Tafel-slope (ca. 0.5 V/dec) region at low overpotential followed by a transition to a highly actively state where the current approaches the diffusion-limiting current; the potential where the transition to the active state occurs decreases with decreasing CO concentration, and the current in the low-overpotential region is roughly inverse half-order in the CO partial pressure. The magnitude of the current in the low-overpotential region on the $Pt_{75}Mo_{25}$ alloy is nearly the same as on the $Pt_{50}Ru_{50}$ alloy, but the potential for the transition to the active state is about 0.15 V higher. The magnitude of the current at 0.05-0.1 V with H_2 containing 100 ppm CO is sufficiently high that Pt-Mo alloy is of technical interest as an anode catalyst for low-

temperature fuel cells fed with a reformed hydrocarbon fuel.

Studies of CO tolerance in low-temperature acid fuel cells will continue by investigating the fundamental aspects of the interaction of CO with the two Pt alloy surfaces, Pt-Mo and Pt-Sn, by FTIR. The examination of methanol oxidation on one or more new Pt alloy systems will also be conducted.

PUBLICATIONS

H. Gasteiger, N. Markovic and P. Ross, "A Remarkable Structure Sensitivity in the Electrooxidation of Carbon Monoxide on Pt_3Sn Alloy Surfaces," *Catal. Lett.* **36**, 1 (1996).

K. Wang, H. Gasteiger, N. Markovic and P. Ross, "On the Reaction Pathway for Methanol and Carbon Monoxide Oxidation on Pt-Sn Versus Pt-Ru Alloy Surfaces," *Electrochim. Acta*, **41**, 2587 (1996).

N. Markovic, H. Gasteiger and P. Ross, "Oxygen Reduction on Platinum Low Index Single Crystal Surfaces in Alkaline Solution: Rotating Ring-Pt(hkl) Disk Studies," *J. Phys. Chem.*, **100**, 6715 (1996).

N. Markovic, S. Sarraf, H. Gasteiger and P. Ross, "Hydrogen Electrochemistry on Pt(hkl) Surfaces in Alkaline Solution," *J. Chem. Soc. Faraday Trans.*, **92**, 3719 (1996).

A. Widelov, N. Markovic and P. Ross, "Electrochemical and Surface Spectroscopic Studies of Thin Films of Bismuth Ruthenium Oxide ($Bi_2Ru_2O_7$)," *J. Electrochem. Soc.*, **143**, 3504 (1996).

Fuel Cell Electrocatalyst and Electrolyte Studies

Elton J. Cairns
70-108B, Lawrence Berkeley National Laboratory, Berkeley CA 94720
(510) 486-5028, fax: (510) 486-7303

Objectives

- Obtain information on the nature of the poisoning intermediate(s) in CH_3OH electrooxidation on Pt-based electrocatalysts by NMR and photothermal deflection spectroscopy (PDS).
- Evaluate novel electrode-electrolyte combinations.

Approach

- Apply NMR and PDS to obtain information about surface poisoning on Pt supported on graphite and Pt anodes in electrolytes containing methanol.
- Carry out gas-diffusion electrode studies in model fuel cells.

Accomplishment

- Major advances were made in eliminating the unwanted coupling of the NMR sample to the coil, thereby permitting the acquisition of meaningful NMR spectra under open-circuit conditions and strongly suggesting the possibility of acquiring spectra under conditions of *in situ* electrode potential control.

Future Direction

- Proceed with more in-depth investigations to acquire quality NMR spectra of electrochemical systems.

The performance of the electrodes employed in direct methanol fuel cells (DMFCs) is typically limited by slow electrochemical kinetics. The goals of research performed on these electrodes are to characterize their kinetic and mechanistic behavior and to identify electrode structures, electrocatalysts, and electrolyte compositions that lead to improved cell performance.

The application of NMR to electrocatalytic systems presents major experimental challenges. Paramount among these is dealing with the conflicting requirements of the two systems with regard to sample conductivity. Electrochemical systems necessarily contain components of high ionic or electronic conductivity, whereas high conductivity in an NMR sample impedes the acquisition of meaningful spectra. We have previously attempted to alleviate this problem by using a porous separator rolled parallel with the electrode, the idea being to eliminate conduction paths in the specific direction that adversely affects the NMR, while preserving the necessary bulk conductivity of the electrochemical system. While this early modification permitted the acquisition of ^{13}CO spectra, they were generally of poor quality and required long acquisition times.

Major advances were made in dealing with the problem of bulk sample conductivity. Through refinement of the electrode-separator structure in conjunction with the inclusion of a non-porous separator, the unwanted coupling of the NMR sample to the coil has been virtually eliminated, thereby permitting the acquisition of meaningful NMR spectra under open-circuit conditions and strongly suggesting the possibility of acquiring spectra under conditions of *in situ* electrode potential control. Using this improved electrode structure, quantitative solid-state NMR spectra of CO adsorbed from solution onto a commercial fuel-cell electrode material have been acquired. Figure 30 shows representative ^{13}CO NMR data. Spectrum A shows the sample with saturation coverage of CO, and spectrum B shows the same sample with no CO adsorbed. The latter spectrum is a background signal and is consistent with the known NMR parameters of graphite (the electrode support material) and PTFE (from probe components). Spectra C-I show background-subtracted data for CO adsorption at different coverages.

NMR data in C-I represent 25,000 acquisitions with a 750 Hz line broadening used to present the Fourier-transformed spectra. Data upfield of 180 ppm represent inadequate background subtraction of PTFE probe components (due to varying alignment of the probe assembly in the NMR coil after each oxidation) and dissolved CO_2 in the aqueous phase.

Previously reported NMR spectra of adsorbed CO from the gas phase onto supported-Pt particles are broad and featureless. Chemical and Knight shifts account for the observed resonance frequencies, whereas line widths are governed by three factors: multiple shifts resulting from a distribution of spins between linear and bridged adsorbates; the large anisotropy of the ^{13}C chemical shift tensors; and further broadening of the chemical shift powder pattern by the large magnetic susceptibility of the metal particles. While our data appear featureless at high coverages, they undergo significant changes as surface coverage decreases; indeed at low coverages the observed line shape is well fit to a chemical shift powder pattern having an anisotropy of about 100 ppm, virtually identical to the anisotropies reported for bridge-bonded CO on supported Ru and Rh particles. Thus our observations appear to be consistent with changing populations of linear and bridge-bonded CO with surface coverage.

PUBLICATION

M.S. Yahnke, B.M. Rush, J.A. Reimer and E.J. Cairns, "Quantitative Solid-State NMR Spectra of CO Adsorbed from Aqueous Solution onto a Commercial Electrode," *J. Am. Chem. Soc.* **118**(48), 12250 (1996).

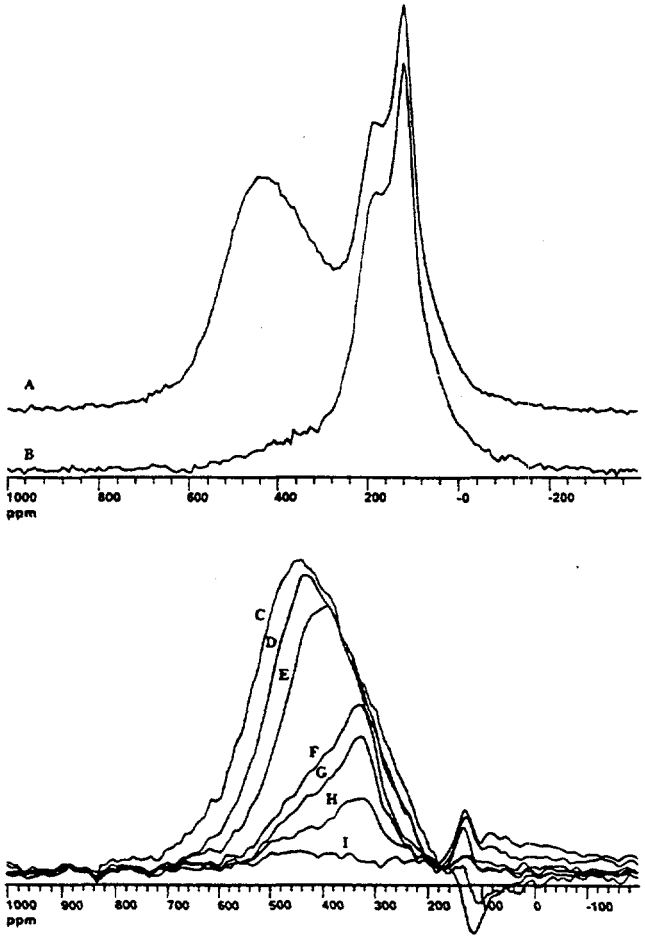

Figure 30. Carbon-13 NMR spectra of Pt/C electrodes. (A) Electrode with saturation coverage of ^{13}CO. (B) Electrode with no CO adsorbed. (C-I). Spectra obtained as a function of ^{13}CO coverage after background subtraction.

Fuel Cells for Renewable Applications

Shimshon Gottesfeld
Los Alamos National Laboratory, MS D429, P.O. Box 1663, Los Alamos NM 87545
(505) 667-0853, fax: (505) 665-4292

Objectives

- Identify, evaluate and initiate development of fuel cell technology for transportation applications.
- Conduct basic research in electrochemistry to explore and improve the potential of fuel cell systems for use in transportation applications.

Approach

- Apply electrocatalysis and heterogeneous catalysis principles to develop improved electrode materials for polymer electrolyte fuel cells (PEFCs).
- Utilize experimental techniques to determine the transport properties of polymer electrolyte membranes.
- Test laboratory-scale fuel cells to obtain information on the performance of cell components.

Accomplishments

- A proof of concept for using the hydrophilic domains in a composite backing material for membrane-electrode assemblies (MEAs) was demonstrated.
- The methanol cross-over rate was lowered (at 80°C) from 110 mA_{eq}/cm^2 through a standard Nafion® 117 membrane to 40 mA_{eq}/cm^2 by use of an alternative membrane.
- It has been demonstrated that continuous stable operation of DMFCs for 500 h is achievable by modifying the cathode structure.

Future Directions

- Continue studies of tolerance to higher levels of CO on PEFCs.
- Continue effort to fabricate molded, flexible, 2-mm thick bipolar plates with imprinted flow fields of minimized overall resistance in the cell and minimized hydrogen permeability.
- Demonstrate new humidification scheme for stack cooling.

The primary focus of this program is to develop efficient and cost-effective PEFC for transportation applications. The specific goals of the program are to: *i)* reduce the cost of the Pt catalyst and ionomeric membrane, *ii)* increase the efficiency and power density of the PEFC, *iii)* optimize the system for operation on reformed organic fuels and air, *iv)* achieve stable, efficient, long-term operation, and *v)* solve key technical issues that impede the development of the DMFC.

Improved CO Tolerance and Fuel Stream Cleanup. Significant advances were made in demonstrating enhanced CO tolerance in PEFCs by combining three elements: *i)* use of PtRu anode catalysts of various types and loadings; *ii)* increasing cell temperature over 80°C; *iii)* bleeding of small levels of air into the anode feed stream

With these combined tools for the enhancement of CO tolerance in PEFCs, we have managed to demonstrate tolerance to 100 ppm CO in the full current density range of the PEFC in long-term tests of several hundred hour duration, and tolerance to 500 ppm CO in shorter tests. In addition to probing and correcting for the deleterious effects of low CO levels, the impurity testing efforts were extended to include effects of traces of ammonia, suspected of being generated in high temperature autothermal fuel processors. The significant deleterious effects at ppm levels of ammonia was confirmed, pointing to the further strong need of impurity tolerance improvement in PEFCs operated on fuel feed streams generated by reforming of liquid hydrocarbons.

The conceptual design and fabrication of a variable flow PROX unit for an anode clean-up system for ultimate integration with a gasoline reformer are underway. In support of this effort the effect of anode gas dilution on the performance was evaluated. The results of this evaluation have been very significant in highlighting potential losses ranging between 25 mV around 0.5 A/cm^2 and

100 mV around 1A/cm² as a result of hydrogen dilution to the level expected in fuel processing by a gasoline reformer.

Low-Cost, High-Performance Stack Materials. The severe combined cost/performance demands from a PEFC stack in transportation applications directs efforts of stack development to non-machined bipolar plate/flow field structures of low intrinsic cost and of potential for achieving high power density. The direction has been to produce a carbon/plastic composite by molding, with the combined properties of high electronic conductivity and mechanical strength and flexibility enabling fabrication of thin, mechanically robust bipolar plate/flow field elements.

The effort is to obtain better mechanical properties with graphite/kynar composites by adding carbon fiber and carbon powder components and by changing the composition in a wide range. The results to date have been promising in terms of improved materials properties of electronic conductivity, gas impermeability and mechanical strength/flexibility. We achieved the following materials characteristics: *i)* bulk conductivity of 100 S/cm; *ii)* hydrogen permeability of less than 0.1 mA_{eq}/cm^2; *iii)* mechanical strength/flexibility superior to that of commercial graphite/kynar plates.

A collaboration was started this year with Federal Fabrics and Fibers (FFF) of Andover, MA, devoted to the fabrication at FFF of molded carbon/plastic composites which are subsequently surface treated using a proprietary FFF process to render high surface conductivity – an important prerequisite for minimizing contact resistance in the stack.

Effective MEA Humidification Schemes. It is highly desirable to simplify the humidification scheme in proton exchange membrane fuel cells (PEMFCs) in order to increase power density and simplify overall system design. Drawbacks of present day schemes are derived from the close coupling between reactant gas supply to the stack and effective stack humidification, as reactant gases carry with them the water vapor for membrane humidification. In this project, novel ideas on simplified and effective humidification schemes are being evaluated and demonstrated. We will particularly target demonstration of effective stack operation at low air pressures, which will become much easier to achieve once the humidification function is separated from the gas reactant supply function.

A specific concept has recently been submitted as a patent application by LANL. It is based on the use of an anode backing material with intermixed hydrophilic and hydrophobic domains. A proof of concept for using the hydrophilic domains in such a composite backing material as wicks for liquid water, supplied separately from the gas feed streams was demonstrated. In one mode of water supply, a well-defined small, separate part of the machined flow field served to deliver liquid water through a composite backing with wicking capacity to the membrane/electrode assembly.

Direct Methanol Oxidation Fuel Cells. The work has focused on adapting for DMFCs the catalyst ink technology that was developed and patented for hydrogen/air fuel cells. Our recent results have demonstrated the efficiency of PtRu catalyst layers prepared in this way for DMFC anodes.

An optimized cathode structure for DMFCs was demonstrated which produced high DMFC cathode performance with lowered Pt loadings by use of 60% Pt/C supported catalysts. This composition proved to have optimized "packaging" *vs.* surface area characteristics.

We have also shown that new ways for preparing unsupported PtRu catalysts can lead to enhanced activities (by about 50%) when incorporated in DMFC anodes. Further work on DMFC electrode optimization will include a variety of tasks, based on thin catalyst layers applied to the membrane directly or by decal techniques, aimed at enhanced catalytic activity.

Methanol crossover in the DMFC must be minimized to achieve higher fuel utilization. The methanol cross-over rate was lowered (at 80°C) from 110 mA_{eq}/cm^2 through a standard Nafion® 117 membrane to 40 mA_{eq}/cm^2 through an alternative membrane. At the same time, the power density of the DMFC employing the alternative membrane was also slightly improved.

An important challenge for the DMFC is to demonstrate performance stability on the time scale of 4000-5000 hours. A long-term testing activity, followed by careful analysis of the effects of long-term operation on cell components and their failure mechanisms, is underway. We have identified DMFC *cathode* problems as the main source of performance loss with time of DMFC operating at 80°C and have introduced some cathode modifications that helped stabilize the performance. It has been demonstrated that continuous stable operation of DMFCs for 500 h is achievable by modifying cathode structure.